13
Chemical and Biological Effects of Radiation

13.1
Time Frame for Radiation Effects

To be specific, we describe the chemical changes produced by ionizing radiation in liquid water, which are relevant to understanding biological effects. Mammalian cells are typically ~70–85% water, ~10–20% proteins, ~10% carbohydrates, and ~2–3% lipids.

Ionizing radiation produces abundant secondary electrons in matter. As discussed in Section 5.3, most secondary electrons are produced in water with energies in the range ~10–70 eV. The secondaries slow down very quickly ($\lesssim 10^{-15}$ s) to subexcitation energies; that is, energies below the threshold required to produce electronic transitions (~7.4 eV for liquid water). Various temporal stages of radiation action can be identified, as we now discuss. The time scale for some important radiation effects, summarized in Table 13.1, covers over 20 orders of magnitude.

13.2
Physical and Prechemical Chances in Irradiated Water

The initial changes produced by radiation in water are the creation of ionized and excited molecules, H_2O^+ and H_2O^*, and free, subexcitation electrons. These species are produced in $\lesssim 10^{-15}$ s in local regions of a track. Although an energetic charged particle may take longer to stop (Sections 5.11 and 6.6), we shall see that portions of the same track that are separated by more than ~0.1 μm develop independently. Thus we say that the initial physical processes are over in $\lesssim 10^{-15}$ s in local track regions.

The water begins to adjust to the sudden physical appearance of the three species even before the molecules can more appreciably in their normal thermal agitation. At room temperature, a water molecule can move an average distance of ~1–2 Å, roughly equal to its diameter (2.9 Å), in ~10^{-12} s. Thus, 10^{-12} s after passage of a charged particle marks the beginning of the ordinary, diffusion-controlled chemical reactions that take place within and around the particle's path. During this prechemical stage, from ~10^{-15} s to ~10^{-12} s, the three initial species produced

Atoms, Radiation, and Radiation Protection. James E. Turner

ISBN: 978-3-527-40606-7

Table 13.1 Time Frame for Effects of Ionizing Radiation

Times	Events
Physical stage	Formation of H_2O^+, H_2O^*, and subexcitation electrons,
$\lesssim 10^{-15}$ s	e^-, in local track regions ($\lesssim 0.1\ \mu$m)
Prechemical stage	Three initial species replaced by H_3O^+, OH, e^-_{aq}, H,
$\sim 10^{-15}$ s to $\sim 10^{-12}$ s	and H_2
Chemical stage	The four species H_3O^+, OH, e^-_{aq}, and H diffuse and
$\sim 10^{-12}$ s to $\sim 10^{-6}$ s	either react with one another or become widely separated. Intratrack reactions essentially complete by $\sim 10^{-6}$ s
Biological stages	
$\lesssim 10^{-3}$ s	Radical reactions with biological molecules complete
$\lesssim 1$ s	Biochemical changes
Minutes	Cell division affected
Days	Gastrointestinal and central nervous system changes
Weeks	Lung fibrosis develops
Years	Cataracts and cancer may appear; genetic effects in offspring

by the radiation induce changes as follows. First, in about 10^{-14} s, an ionized water molecule reacts with a neighboring molecule, forming a hydronium ion and a hydroxyl radical:

$$H_2O^+ + H_2O \rightarrow H_3O^+ + OH. \tag{13.1}$$

Second, an excited water molecule gets rid of its energy either by losing an electron, thus becoming an ion and proceeding according to the reaction (13.1), or by molecular dissociation:

$$H_2O^* \rightarrow \begin{cases} H_2O^+ + e^- \\ H + OH \end{cases}. \tag{13.2}$$

The vibrational periods of the water molecule are $\sim 10^{-14}$ s, which is the time that characterizes the dissociation process. Third, the subexcitation electrons migrate, losing energy by vibrational and rotational excitation of water molecules, and become thermalized by times $\sim 10^{-12}$ s. Moreover, the thermalized electrons orient the permanent dipole moments of neighboring water molecules, forming a cluster, called a hydrated electron. We denote the thermalization–hydration process symbolically by writing

$$e^- \rightarrow e^-_{aq}, \tag{13.3}$$

where the subscript aq refers to the fact that the electron is hydrated (aqueous solution). These changes are summarized for the prechemical stage in Table 13.1. Of the five species formed, H_2 does not react further.

13.3 Chemical Stage

At $\sim 10^{-12}$ s after passage of a charged particle in water, the four chemically active species H_2O^+, OH, e^-_{aq}, and H are located near the positions of the original H_2O^+, H_2O^*, and e^- that triggered their formation. Three of the new reactants, OH, e^-_{aq}, and H, are free radicals, that is, chemical species with unpaired electrons. The reactants begin to migrate randomly about their initial positions in thermal motion. As their diffusion in the water proceeds, individual pairs can come close enough to react chemically. The principal reactions that occur in the track of a charged particle in water during this stage are the following:

$$OH + OH \rightarrow H_2O_2, \tag{13.4}$$

$$OH + e^-_{aq} \rightarrow OH^-, \tag{13.5}$$

$$OH + H \rightarrow H_2O, \tag{13.6}$$

$$H_3O^+ + e^-_{aq} \rightarrow H + H_2O, \tag{13.7}$$

$$e^-_{aq} + e^-_{aq} + 2H_2O \rightarrow H_2 + 2OH^-, \tag{13.8}$$

$$e^-_{aq} + H + H_2O \rightarrow H_2 + OH^-, \tag{13.9}$$

$$H + H \rightarrow H_2. \tag{13.10}$$

With the exception of (13.7), all of these reactions remove chemically active species, since none of the products on the right-hand sides except H will consume additional reactants. As time passes, the reactions (13.4)–(13.10) proceed until the remaining reactants diffuse so far away from one another that the probability for additional reactions is small. This occurs by $\sim 10^{-6}$ s, and the chemical development of the track in pure water then is essentially over.

The motion of the reactants during this diffusion-controlled chemical stage can be viewed as a random walk, in which a reactant makes a sequence of small steps in random directions beginning at its initial position. If the measured diffusion constant for a species is D, then, on the average, it will move a small distance λ in a time τ such that

$$\frac{\lambda^2}{6\tau} = D. \tag{13.11}$$

Each type of reactive species can be regarded as having a reaction radius R. Two species that approach each other closer than the sum of the their reactive radii have a chance to interact according to Eqs. (13.4)–(13.10). Diffusion constants and reaction radii for the four reactants in irradiated water are shown in Table 13.2.

Example

Estimate how far a hydroxyl radical will diffuse in 10^{-12} s.

Table 13.2 Diffusion Constants D and Reaction Radii R for Reactive Species

Species	D (10^{-5} cm^2 s^{-1})	R (Å)
OH	2	2.4
e^-_{aq}	5	2.1
H_3O^+	8	0.30
H	8	0.42

Solution

From Eq. (13.11) with $\tau = 10^{-12}$ s and from Table 13.2, we find

$$\lambda = (6\tau D)^{1/2} = (6 \times 10^{-12}\ \text{s} \times 2 \times 10^{-5}\ \text{cm}^2\ \text{s}^{-1})^{1/2}$$
$$= 1.10 \times 10^{-8}\ \text{cm} = 1.10\ \text{Å}. \tag{13.12}$$

For comparison, the diameter of the water molecule is 2.9 Å. The answer (13.12) is compatible with our taking the time $\sim 10^{-12}$ s as marking the beginning of the chemical stage of charged-particle track development.

13.4 Examples of Calculated Charged-Particle Tracks in Water

Before discussing the biological effects of radiation we present some examples of detailed calculations of charged-particle tracks in water. The calculations have been made from the beginning of the physical stage through the end of the chemical stage.

Monte Carlo computer codes have been developed for calculating the passage of a charged particle and its secondaries in liquid water. In such computations, an individual particle is allowed to lose energy and generate secondary electrons on a statistical basis, as it does in nature. Where available, experimental values of the energy-loss cross sections are used in the computations. The secondary electrons are similarly transported and are allowed to produce other secondary electrons until the energies of all secondaries reach subexcitation levels (<7.4 eV). Such calculations give in complete detail the position and identity of every reactant H_2O^+, H_2O^*, and subexcitation electron present along the track. These species are allowed to develop according to (13.1), (13.2), and (13.3) to obtain the positions and identities of every one of the reactive species OH, H_3O^+, e^-_{aq}, and H at 10^{-12} s. The computations then carry out a random-walk simulation of diffusion by letting each reactant take a small jump in a random direction and then checking all pairs to see which are closer than the sum of their reaction radii. Those that can react do so and are removed from further consideration [except when H is produced by (13.7)]. The remainder are jumped again from their new positions and the procedure is repeated to develop the track to later times. The data in Table 13.2 and the reaction

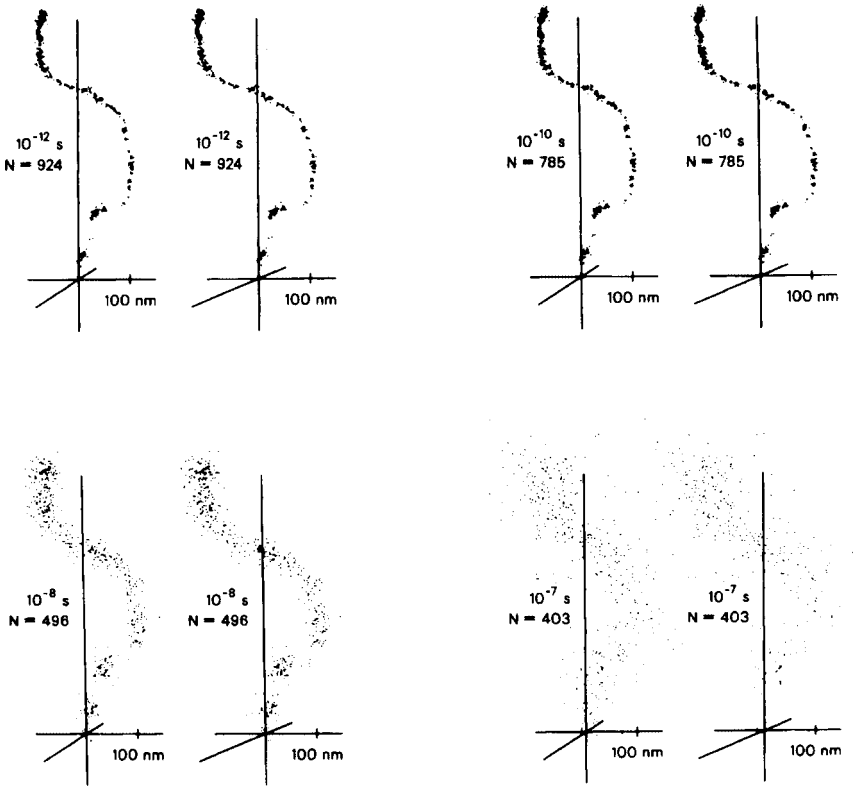

Fig. 13.1 Chemical development of a 4-keV electron track in liquid water, calculated by Monte Carlo simulation. Each dot in these stereo views gives the location of one of the active radiolytic species, OH, H_3O^+, e^-_{aq}, or H, at the times shown. Note structure of track with spurs, or clusters of species, at early times. After 10^{-7} s, remaining species continue to diffuse further apart, with relatively few additional chemical reactions. (Courtesy Oak Ridge National Laboratory, operated by Martin Marietta Energy Systems, Inc., for the Department of Energy.)

schemes (13.4)–(13.10) can thus be used to carry out the chemical development of a track.

Three examples of calculated electron tracks at 10^{-12} s in liquid water were shown in Fig. 6.5. The upper left-hand panel in Fig. 13.1 presents a stereoscopic view of another such track, for a 4-keV electron, starting at the origin in the upward direction. Each dot represents the location of one of the active radiolytic species, OH, H_3O^+, e^-_{aq}, or H, shown in Table 13.2, at 10^{-12} s. There are 924 species present initially. The electron stops in the upper region of the panel, where its higher linear energy transfer (LET) is evidenced by the increased density of dots. The occurrence of species in clusters, or spurs, along the electron's path is seen. As discussed in Section 6.7, this important phenomenon for the subsequent chemical action of ionizing radiation is a result of the particular shape and universality of the energy-loss spectrum for charged particles (Fig. 5.3). The passage of time and the chemical

reactions within the track are simulated by the procedures described in the last paragraph. The track is shown at three later stages in Fig. 13.1. At 10^{-7} s, the number of reactive species has decreased to 403, and the original structure of the track itself has largely disappeared. Relatively few subsequent reactions take place as the remaining species diffuse ever more widely apart.

A 1-μm segment of the track of a 2-MeV proton, traveling from left to right in liquid water, is shown in Fig. 13.2, calculated to 2.8×10^{-7} s. In contrast to the 4-keV electron in the last figure, the proton track is virtually straight and its high LET leads to a dense formation of reactants along its path. The relative reduction in the number of reactants and the disappearance of the details of the original track structure by 2.8×10^{-7} s are, however, comparable. This similarity is due to the fact that intratrack chemical reactions occur only on a local scale of a few hundred angstroms or less, as can be inferred from Figs. 13.1 and 13.2. Separate track segments of this size develop independently of other parts of the track.

These descriptions are borne out by closer examination of the tracks. The middle one-third of the proton track at 10^{-11} s in Fig. 13.2 is reproduced on a blown-up scale in the upper line of Fig. 13.3. The second line in this figure shows this segment at 2.8×10^{-9} s, as it develops independently of the rest of the track. On an even more expanded scale, the third and fourth lines in Fig. 13.3 show the last third of the track segment from the top line of the figure at 10^{-11} s and 2.8×10^{-9} s. The scale 0.01 μm = 100 Å indicates that most of the chemical development of charged-particle tracks takes place within local regions of a few hundred angstroms or less.

Figure 7.1 showed four examples of 0.7-μm segments of the tracks of protons and alpha particles, having the same velocities, at 10^{-11} s. Fast heavy ions of the same velocity have almost the same energy-loss spectrum. Because it has two units of charge, the linear rate of energy loss (stopping power) for an alpha particle is four times that of a proton at the same speed (cf. Section 5.6). Thus the LET of the alpha particles is about four times that of the protons at each energy.

13.5
Chemical Yields in Water

When performing such calculations for a track, the numbers of various chemical species present (e.g., OH, e^-_{aq}, H_2O_2, etc.) can be tabulated as functions of time. These chemical yields are conveniently expressed in terms of *G* values—that is, the number of a given species produced per 100 eV of energy loss by the original charged particle and its secondaries, on the average, when it stops in the water. Calculated chemical yields can be compared with experimental measurements. To obtain adequate statistics, computations are repeated for a number of different, independent tracks and the average *G* values are compiled. As seen from reactions (13.4)–(13.10), *G* values for the reactant species decrease with time. For example, hydroxyl radicals and hydrated electrons are continually used up, while *G* values for

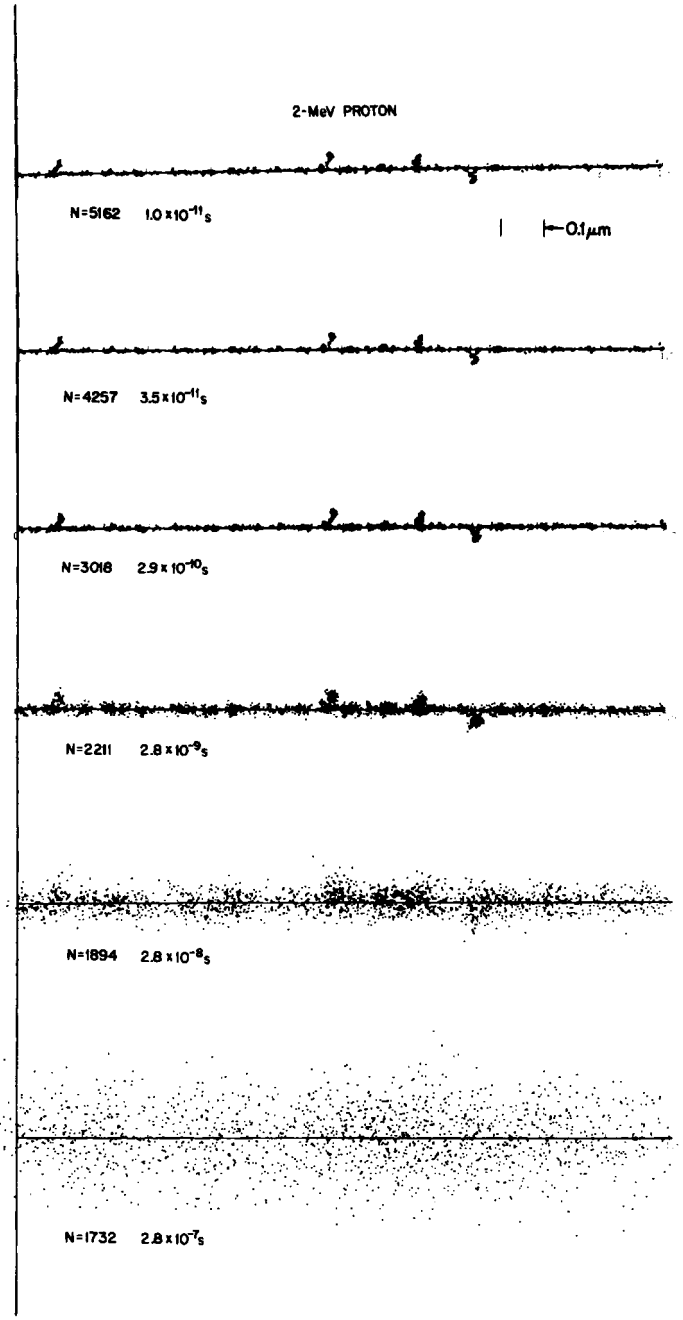

Fig. 13.2 Development of a 1-μm segment of the track of a 2-MeV proton, traveling from left to right, in liquid water. (Courtesy Oak Ridge National Laboratory, operated by Martin Marietta Energy Systems, Inc., for the Department of Energy.)

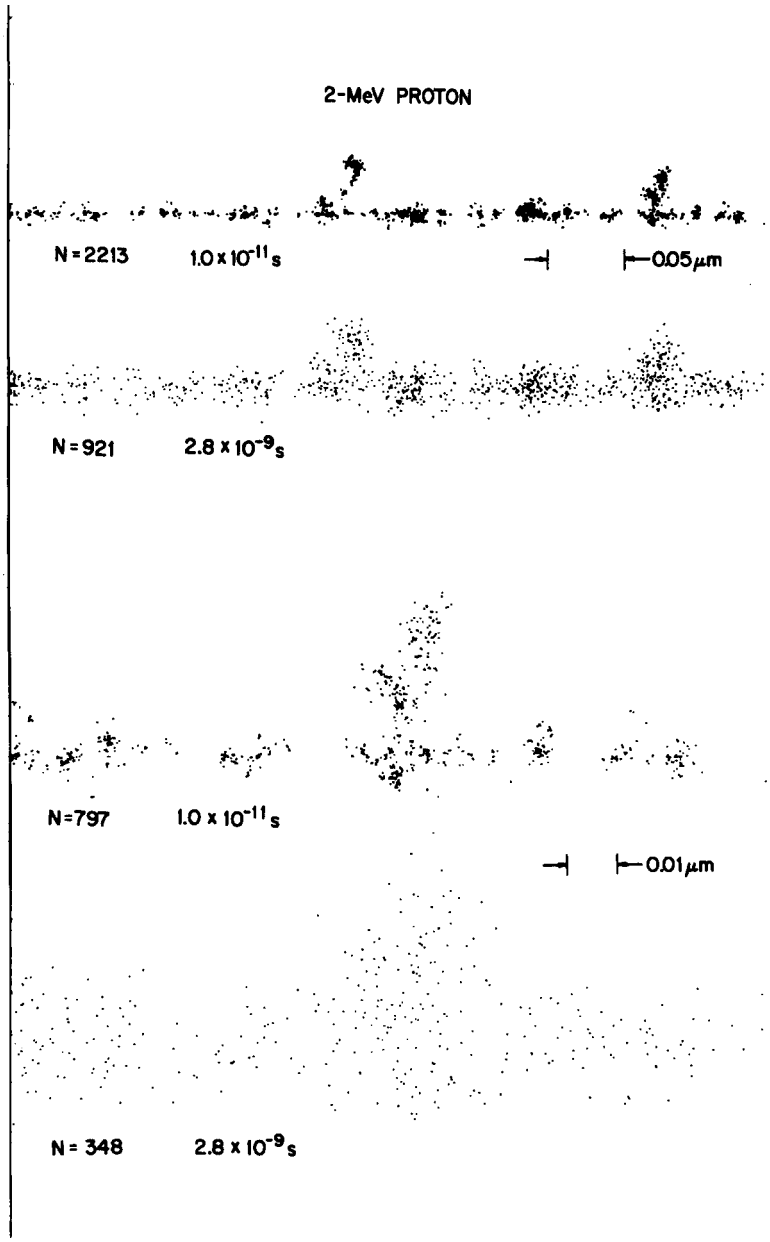

Fig. 13.3 Magnified view of the middle one-third of the track segment from Fig. 13.2 at 10^{-11} s and at 2.8×10^{-9} s is shown in the upper two lines. The two lower lines show the right-hand third of this segment at these times under still greater magnification. The figures illustrate how most of the chemical development of charged-particle tracks in pure water takes place in local regions of a few hundred angstroms or less in a track. (Courtesy Oak Ridge National Laboratory, operated by Martin Marietta Energy Systems, Inc., for the Department of Energy.)

Table 13.3 *G* Values (Number per 100 eV) for Various Species in Water at 0.28 μs for Electrons at Several Energies

	Electron Energy (eV)							
Species	**100**	**200**	**500**	**750**	**1000**	**5000**	**10,000**	**20,000**
OH	1.17	0.72	0.46	0.39	0.39	0.74	1.05	1.10
H_3O^+	4.97	5.01	4.88	4.97	4.86	5.03	5.19	5.13
e^-_{aq}	1.87	1.44	0.82	0.71	0.62	0.89	1.18	1.13
H	2.52	2.12	1.96	1.91	1.96	1.93	1.90	1.99
H_2	0.74	0.86	0.99	0.95	0.93	0.84	0.81	0.80
H_2O_2	1.84	2.04	2.04	2.00	1.97	1.86	1.81	1.80
Fe^{3+}	17.9	15.5	12.7	12.3	12.6	12.9	13.9	14.1

the other species, such as H_2O_2 and H_2, increase with time. As mentioned earlier, by about 10^{-6} s the reactive species remaining in a track have moved so far apart that additional reactions are unlikely. As functions of time, therefore, the *G* values change little after 10^{-6} s.

Calculated yields for the principal species produced by electrons of various initial energies are given in Table 13.3. The *G* values are determined by averaging the product yields over the entire tracks of a number of electrons at each energy. [The last line, for Fe^{3+}, applies to the Fricke dosimeter (Section 10.6). The measured *G* value for the Fricke dosimeter for tritium beta rays (average energy 5.6 keV), is 12.9.] The table indicates how subsequent changes induced by radiation can be partially understood on the basis of track structure—an important objective in radiation chemistry and radiation biology. One sees that the *G* values for the four reactive species (the first four lines) are smallest for electrons in the energy range 750–1000 eV. In other words, the intratrack chemical reactions go most nearly to completion for electrons at these initial energies. At lower energies, the number of initial reactants at 10^{-12} s is smaller and diffusion is more favorable compared with reaction. At higher energies, the LET is less and the reactants at 10^{-12} s are more spread out than at 750–1000 eV, and thus have a smaller probability of subsequently reacting.

Similar calculations have been carried out for the track segments of protons and alpha particles. The results are shown in Table 13.4. As in Fig. 7.1, pairs of ions have the same speed, and so the alpha particles have four times the LET of the protons in each case. Several findings can be pointed out. First, for either type of particle, the LET is smaller at the higher energies and hence the initial density of reactants at 10^{-12} s is smaller. Therefore, the efficiency of the chemical development of the track should get progressively smaller at the higher energies. This decreased efficiency is reflected in the increasing *G* values for the reactant species in the first four lines (more are left at 10^{-7} s) and in the decreasing *G* values for the reaction products in the fifth and sixth lines (fewer are produced). Second, at a given velocity, the reaction efficiency is considerably greater in the track of an alpha particle than in the track of a proton. Third, comparison of Tables 13.3 and 13.4 shows some

Table 13.4 *G* Values (Number per 100 eV) for Various Species at 10^{-7} s for Protons of Several Energies and for Alpha Particles of the Same Velocities

Species	Protons (MeV)				Alpha Particles (MeV)			
Type	1	2	5	10	4	8	20	40
OH	1.05	1.44	2.00	2.49	0.35	0.66	1.15	1.54
H_3O^+	3.53	3.70	3.90	4.11	3.29	3.41	3.55	3.70
e^-_{aq}	0.19	0.40	0.83	1.19	0.02	0.08	0.25	0.46
H	1.37	1.53	1.66	1.81	0.79	1.03	1.33	1.57
H_2	1.22	1.13	1.02	0.93	1.41	1.32	1.19	1.10
H_2O_2	1.48	1.37	1.27	1.18	1.64	1.54	1.41	1.33
Fe^{3+}	8.69	9.97	12.01	13.86	6.07	7.06	8.72	10.31

overlap and some differences in yields between electron tracks and heavy-ion track segments. At the highest LET, the reaction efficiency in the heavy-ion track is much greater than that for electrons of any energy.

Electrons, protons, and alpha particles all produce the same species in local track regions at 10^{-15} s: H_2O^+, H_2O^*, and subexcitation electrons. The chemical differences that result at later times are presumably due to the different spatial patterns of initial energy deposition that the particles have.

13.6 Biological Effects

It is generally assumed that biological effects on the cell result from both direct and indirect action of radiation. Direct effects are produced by the initial action of the radiation itself and indirect effects are caused by the later chemical action of free radicals and other radiation products. An example of a direct effect is a strand break in DNA caused by an ionization in the molecule itself. An example of an indirect effect is a strand break that results when an OH radical attacks a DNA sugar at a later time (between $\sim 10^{-12}$ s and $\sim 10^{-9}$ s). The difference between direct and indirect effects is illustrated by Fig. 13.4. The dots in the helical configuration schematically represent the location of sugars and bases on a straight segment of DNA 200 Å in length in water. The cluster of dots mostly to the right of the helix gives the positions of the reactants at 10^{-11} s and the subsequent times shown after passage of a 5-keV electron along a line perpendicular to the page 50 Å from the center of the axis of the helix.

In addition to any transitions produced by the initial passage of the electron or one of its secondaries (direct effects), the reactants produced in the water can attack the helix at later times (indirect effects). In these computations, the electron was made to travel in a straight line. Also, unreacted radicals were assigned a fixed probability per unit time of simply disappearing, in order to simulate scavenging

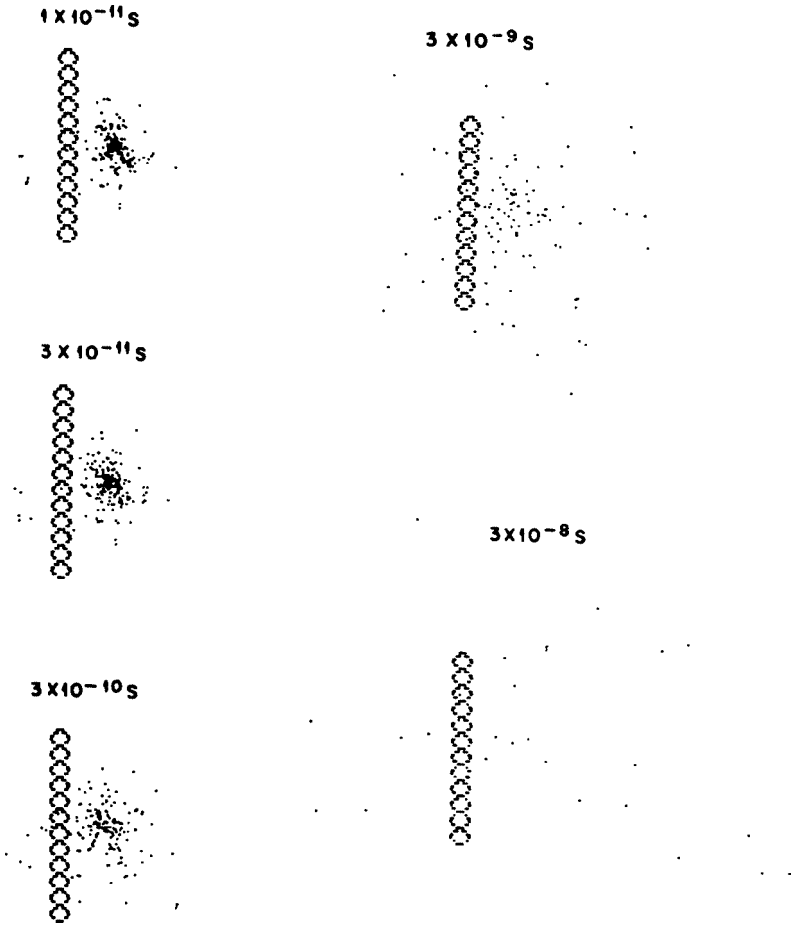

Fig. 13.4 Direct and indirect action of radiation. Double-helical array of dots represents positions of bases and sugars on a 200-Å straight segment of double-stranded DNA. The other dots show the positions of reactants formed in neighboring water from 10^{-11} s to 3×10^{-8} s after passage of a 5-keV electron perpendicular to the page in a straight line 50 Å from the center of the helix. In addition to any direct action (i.e., quantum transitions) produced in the DNA by passage of the electron, indirect action also occurs later when the reactants diffuse to the DNA and react with it. Reactants can also disappear by scavenging in this example, crudely simulating a cellular environment. See text. (Courtesy H. A. Wright and R. N. Hamm, Oak Ridge National Laboratory, operated by Martin Marietta Energy Systems, Inc., for the Department of Energy.)

in a cellular environment. Thus, reactants disappear at a much faster rate here than in the previous examples for pure water.

Depending on the dose, kind of radiation, and observed endpoint, the biological effects of radiation can differ widely. Some occur relatively rapidly while others may take years to become evident. Table 13.1 includes a summary of the time scale for some important biological effects caused by ionizing radiation. Probably by

about 10^{-3} s, radicals produced by a charged-particle track in a biological system have all reacted. Some biochemical processes are altered almost immediately, in less than about 1 s. Cell division can be affected in a matter of minutes. In higher organisms, the time at which cellular killing becomes expressed as a clinical syndrome is related to the rate of cell renewal. Following a large, acute, whole-body dose of radiation, hematopoietic death of an individual might occur in about a month. A higher dose could result in earlier death (1 to 2 wk) from damage to the gastrointestinal tract. At still higher doses, in the range of 100 Gy, damage to membranes and to blood vessels in the brain leads to the cerebrovascular syndrome and death within a day or two. Other kinds of damage, such as lung fibrosis, for example, may take several months to develop. Cataracts and cancer occur years after exposure to radiation. Genetic effects, by definition, are first seen in the next or subsequent generations of an exposed individual.

The biological effects of radiation can be divided into two general categories, stochastic and deterministic, or nonstochastic. As the name implies, stochastic effects are those that occur in a statistical manner. Cancer is one example. If a large population is exposed to a significant amount of a carcinogen, such as radiation, then an elevated incidence of cancer can be expected. Although we might be able to predict the magnitude of the increased incidence, we cannot say which particular individuals in the population will contract the disease and which will not. Also, since there is a certain natural incidence of cancer without specific exposure to radiation, we will not be completely certain whether a given case was induced or would have occurred without the exposure. In addition, although the expected incidence of cancer increases with dose, the severity of the disease in a stricken individual is not a function of dose. In contrast, deterministic effects are those that show a clear causal relationship between dose and effect in a given individual. Usually there is a threshold below which no effect is observed, and the severity increases with dose. Skin reddening is an example of a deterministic effect of radiation.

Stochastic effects of radiation have been demonstrated in man and in other organisms only at relatively high doses, where the observed incidence of an effect is not likely due to a statistical fluctuation in the normal level of occurrence. At low doses, one cannot say with certainty what the risk is to an individual. As a practical hypothesis, one usually assumes that any amount of radiation, no matter how small, entails some risk. However, there is no agreement among experts on just how risk varies as a function of dose at low doses. We shall return to this subject in Section 13.13 in discussing dose–response relationships.

We outline next some of the principal sources of data on the effects of radiation on humans and then describe the effects themselves. This collective body of information, which we only briefly survey here, represents the underlying scientific basis for the radiation-protection standards, criteria, and limits that have been developed. Additional information can be obtained from the references listed in Section 13.15. Virtually all aspects of standards setting are under continuing evaluation and review.

13.7 Sources of Human Data

A considerable body of data exists on radiation effects on man. Risks for certain deleterious effects are reasonably well established at high doses, well above recommended limits. Without attempting to be complete, we mention some of the important sources of data on humans to indicate their scope and the kinds of effects encountered. For many years (into the 1950s), the genetic effects of radiation were considered to pose the greatest danger for human populations exposed to low levels of radiation. Today, the major concern is cancer.

The Life Span Study

The most important source of information on the effects of ionizing radiation on humans is the continuing Life Span Study of long-term health effects in the atomic-bomb survivors at Hiroshima and Nagasaki. The work is conducted by the joint Japanese/United-States Radiation Effects Research Foundation[1)] (RERF). Its objectives include the assessment and characterization of differences in life span and causes of death among the atomic-bomb survivors compared with unexposed persons. Incidence and mortality data are obtained from vital-statistics surveys, death certificates, and other sources. The original sample for the study consisted of about 120,000 persons from among approximately 280,000 identified at the time of the 1950 census as having been exposed to the weapons. Included were a core group of survivors exposed within 2 km of ground zero, other survivors exposed out to distances where little radiation was received, and non-exposed individuals. The sample was eventually constructed by sub-sampling to include all members of the core group and equal-sized samples from the other two, matched by age and sex. Various special cohorts have been formed to study particular questions.

A major task was undertaken to assign doses retrospectively to organs of each individual survivor. Doses were based on analysis of what was known about the weapons' output and the location and shielding of the individual. A number of measurements were conducted at the Nevada Test Site and elsewhere in support of this work. By 1965, a tentative dosimetry system, T65D, was in place for estimating individual doses. This system was substantially updated by the 1986 revision, DS86. The basic quantities determined included the gamma and neutron contributions to the free-in-air kerma and the shielded kerma as functions of the ground distance from the detonations. Doses to different tissues and organs were estimated for individual survivors.

Certain discrepancies persisted between some DS86 predictions when compared with important markers. For example, differences were found between calculated neutron activation products and the activity measured in materials actually exposed at different distances to the bomb radiation. (Activation products include

1 Formally called the Atomic Bomb Casualty Commission.

^{152}Eu and ^{154}Eu in rock and concrete, ^{60}Co in steel and granite, ^{36}Cl in granite and concrete, ^{63}Ni in steel, and others). A number of improvements were made in all aspects of the DS86 radiation computations for Hiroshima and Nagasaki. Calculations with newer cross-section values were made of the bomb-released radiation and its air-over-land transport. The greatly advanced capabilities of computers permitted three-dimensional calculations of the detonations and radiation transport. Shielding by terrain and large buildings was upgraded. Differences between predicted and measured activations were resolved under the new dosimetry system, as were other issues. The estimated yield of the Hiroshima weapon (uranium) was revised from 15 to 16 kilotons (TNT), and the epicenter was relocated 20 m higher than before and 15 m to the west. The 21-kiloton yield of the Nagasaki weapon (plutonium) was confirmed with detonation close to its previously assigned site. The new RERF dosimetry system, DS02, has effectively resolved all discrepancies that existed with DS86. Results are now within expected uncertainties for this kind of work. Analysis indicates that the major contribution to the error in doses determined for an individual are the uncertainty in his or her position and orientation at the time of the explosion and the attenuation by surrounding structures. The development of the DS02 system represents a major contribution to the Life Span Study.

Statistically significant excess cancer deaths of the following types have appeared among the atomic-bomb survivors: leukemia; all cancers except leukemia; and cancers of the stomach, colon, lung, female breast, esophagus, ovary, bladder; and multiple myeloma. Mortality data on solid cancer and leukemia were analyzed by using both DS86 and DS02 dose estimates. The new dosimetry system led to only slight revisions in the effects of risk-modifying factors, such as sex, age at exposure, and time since exposure. The risk per unit dose for solid cancers was decreased by about 10%. Leukemia was the first cancer to be linked to radiation exposure among the Japanese survivors. It also has the highest relative risk. The following findings have appeared in some of the approximately 3,000 survivors exposed *in utero*: reduction in IQ with increasing dose, higher incidence of mental retardation among the highly exposed, and some impairment in rate of growth and development.

Statistically significant radiation-related mortality is also seen for non-neoplastic diseases, such as those associated with the heart, respiratory, digestive, and hematopoietic systems. The effects of both cancer and non-cancer mortality are reflected in a general life shortening. The median loss of life in one cohort with estimated doses in the range 0.005 Gy to 1.0 Gy was about 2 months. With doses of 1 Gy or more, the median was about 2.6 years.

Careful searches have been made for genetic effects in the exposed population. Demonstration of such effects is made difficult by the background of naturally occurring spontaneous mutations. Chromosome abnormalities, blood proteins, and other factors have been studied in children born to one or both exposed parents. No significant differences are found in still births, birth weight, sex ratio, infant mortality, or major congenital abnormalities. The Japanese studies indicate, "… that

at low doses the genetic risks are small compared to the baseline risks of genetic diseases."[2)]

With its enormous scope and scientific value, the studies of the Japanese atomic-bomb survivors have certain drawbacks. The numbers of persons in the lower dose ranges are not sufficiently large to provide direct evidence for radiation effects in man below about 0.2 Gy. The findings nevertheless furnish important estimates of upper limits for the risks for certain effects. In the context of radiation-protection limits, the Japanese exposures were acute and provide no information on how responses might differ for protracted exposures over long times at low dose rates. The exposed populations are also lacking in healthy males of military age. Additional confounding factors in the studies include the possible effects of blast and thermal injuries and poor nutrition and medical care following the attacks on the two cities. In addition, a number of the survivors are still alive, these persons being, of course, the youngest at the time of the exposure. Lifetime risk estimates based on the Japanese data thus still reflect projections of what will happen in this group.

Figure 13.5 presents an example of risk estimation for bomb survivors from the Life Span Study. The excess risk (relative to that at zero dose) for solid cancer is shown as a function of dose. These particular data are averaged over sex and standardized to represent survivors exposed at age 30 who have attained age 60. The doses are grouped into ten intervals and plotted as points at the interval midpoints. The error bars through the points approximate 95% confidence intervals. Two fitted curves are shown as alternative mathematical representations of the risk-*vs.*-dose relationship. The inset shows, for comparison, a linear-quadratic fit for leukemia, which shows greater curvature than solid cancer.

For the purpose of establishing radiation-protection criteria for workers and the public, assessments of risk at low doses and dose rates are of primary concern. Experimentally, it is found that a given large dose of radiation, delivered acutely, is generally more damaging biologically than the same dose delivered over an extended period of time (cf., e.g., Fig. 13.17). In the Life Span Study, therefore, the application of *dose and dose-rate effectiveness factors* (DDREFs) are suggested in order to reduce risks as numerically found in the bomb survivors to values deemed more appropriate for exposure at low doses and dose rates. DDREFs for adjusting linear risk estimates are judged to be in the range 1.1 to 2.3, with a median of 1.5 often being applied.

For a comprehensive review and assessment of health risks from exposure to low levels of ionizing radiation, the reader is referred to the 2006 BEIR VII Phase 2 Report (see references in Section 13.15). Virtually all sources of information on human exposures are addressed.

Medical Radiation

Studies have been made of populations exposed to therapeutic and diagnostic radiation. While often lacking the sample size and quality of dosimetry that char-

2 BEIR VII Report, p. 118 (see references, Sect. 13.15).

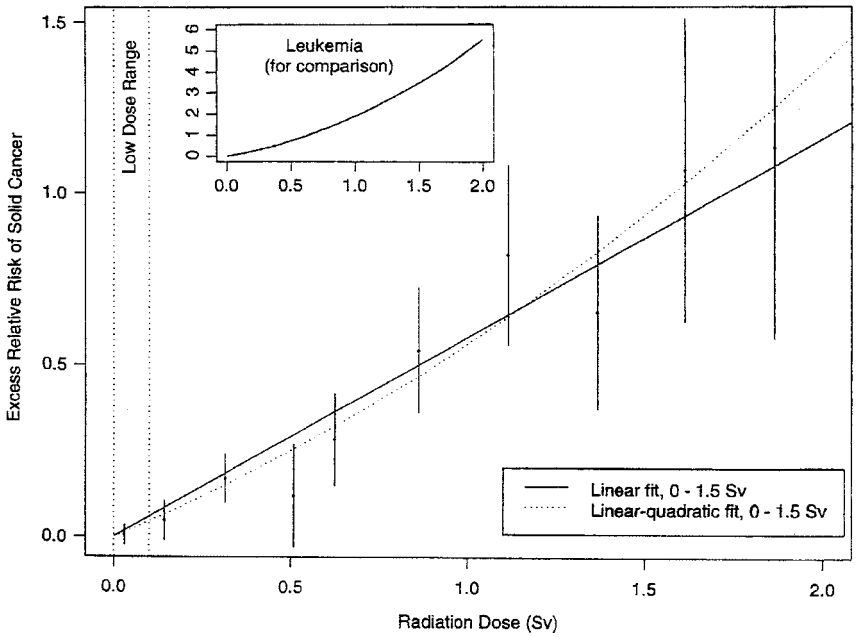

Fig. 13.5 Example from Life Span Study. Excess relative risks of solid cancer for Japanese atomic-bomb survivors exposed at age 30 who attained age 60. Inset shows the fit of a linear-quadratic model for leukemia, to illustrate the greater degree of curvature observed for that cancer. See text. [Reprinted with permission from Health Risks from Exposure to Low Levels of Ionizing Radiation: BEIR VII Phase 2, © (2006) by the National Academy of Sciences, courtesy of the National Academies Press, Washington, DC.]

acterize the Life Span Study, such investigations can provide some insight into issues outside the scope of the Japanese data—for example, protracted exposures. The following three examples illustrate some findings from medical exposures of humans.

First, X rays were used in the 1930s and 1940s to shrink enlarged thymus glands in children. Treatments could deliver a substantial incidental dose to a child's thyroid, one of the most sensitive tissues for cancer induction by radiation. An abnormally large number of benign and malignant thyroid tumors developed later in life among individuals that underwent this procedure as children for treating the thymus.

Second, it was also common in the 1940s and 1950s to use X rays to treat ringworm of the scalp *(tinea capitis)* in children. A dose of several Gy was administered to the scalp to cause (temporary) epilation, so that the hair follicles could be more effectively treated with medicines. This procedure also resulted in a substantial thyroid dose. Following the establishment of the State of Israel, ringworm of the scalp reached epidemic proportions among immigrants coming there from North Africa. Israeli physicians treated over 10,000 immigrating children, who later showed about a sixfold increase in the incidence of malignant thyroid tumors, compared with unirradiated controls. A survey of 2215 patients similarly treated in New

York yielded excess numbers of thyroid adenomas, leukemia, and brain cancer, but no excess thyroid cancer.

A third example of information obtained on radiation effects from medical exposures is derived from the study of some 14,000 patients treated during the 1930s and early 1940s in Great Britain for ankylosing spondylitis. Large doses of X rays were given to the spine to relieve pain caused by this disease. Retrospective examination of patients' records revealed a small, but statistically significant, increase in leukemia as the cause of death. Doses to the active bone marrow and organs in the treatment field were of the order of several Gy. In addition to uncertainties in the dosimetry, the study lacks a satisfactory cohort of controls—patients having the same disease and receiving similar treatment, but without X-ray therapy.

Radium-Dial Painters

Radioluminescent paints, made by combining radium with fluorescent materials, were popular in the 1920s. They were used in the production of watch and clock dials, gun sights, and other applications. The industry was widespread. A hundred or more firms purchased the paint, which was applied, almost exclusively by women, to the dials with small brushes. One company reported turning out about 4,300 dials each day. Figure 13.6 shows a typical dial-painting studio of the time in Illinois. Each painter had her materials on the desk top in front of her, and the finished dials can be seen placed to the right of where she sat.

Fig. 13.6 A studio with radium dial painters, *cir.* 1920s. The proximity of the painted dials at the workers' sides and the supply of radium paint on their desks added an external gamma dose to the internal dose from the ingested radium. [From R. E. Rowland, *Radium in Humans, a Review of U.S. Studies*, Report ANL/ER-3, Argonne National Laboratory, Argonne, IL (1994).]

By the 1920s it was apparent that radiation-related diseases and fatalities were occurring in the industry. The common practice of tipping brushes with the tongue was causing the ingestion of radium, a bone-seeking element, by hundreds of workers. An extensive registry of individual dial painters was subsequently compiled, with information on exposure history. More than 1,000 individuals had their radium body content measured. Bone samples were taken after death and analyzed. An occupational guide of 0.1 μg for the maximum permissible amount of ^{226}Ra in the body was later established, based on the findings of the worker studies. It was estimated that this level corresponds to an average dose rate of 0.6 mGy wk^{-1} and a dose equivalent rate of perhaps between ~1 and ~6 mSv wk^{-1}. We shall return to this baseline level in the next chapter on radiation-protection limits.

Uranium Miners

The experience with uranium miners provides another important body of information on radiation effects in human beings. The data are particularly pertinent to the ubiquitous exposure of persons to the naturally occurring daughters of radon. Dating back to the Middle Ages, it was recognized that miners in some parts of Czechoslovakia and southern Germany had abnormally large numbers of lung disorders, referred to as mountain sickness (Bergkrankheit). Well into the twentieth century, miners were exposed to high concentrations of dusts, containing ores of arsenic, uranium, and other metals. The incidence of lung cancer was elevated—in some locations, 50% of the miners died of this disease. Recognition of the role of radon and its daughters was slow in coming. It has been generally accepted as the principal causative agent for lung cancer among uranium miners for only about the last 60 years.

In 1999 the National Research Council published its comprehensive BEIR VI Report, *Health Effects of Exposure to Radon*, updating the 1988 BEIR IV Report on radon and alpha emitters (see references in Section 13. 15). The records of thousands of uranium miners have been examined and analyzed by many investigators in terms of lung-cancer incidence among workers exposed at various levels throughout the world. Supplemented with extensive laboratory work, models have been developed to compute doses to lung tissues per working level month (WLM, Section 4.6) of exposure to radon daughters. Depending on the particular assumptions made and the lung tissue in question, values are in the range 0.2 to 3.0 mGy (WLM)$^{-1}$.[3)] A cohort of eleven studies involved 60,606 relatively highly exposed miners worldwide. The mean exposure was 164.4 WLM and the mean duration, 5.7 y. There were 2,674 lung-cancer deaths among the exposed individuals. The data were compared with other cohorts, having successively smaller mean exposures, more applicable to estimating risks at low doses and dose rates. Exposures in the epidemiologic studies of miners are about an order of magni-

3 BEIR VI Report, p. 202.

Table 13.5 Estimated Number of Lung-cancer Deaths in 1995 in the U.S. Attributable to Indoor Residential Radon*

Population	Lung-cancer Deaths	Number of Deaths Attributable to Indoor Rn	
		Model 1	Model 2
Total Persons	157,400	21,800	15,400
Ever Smokers	146,400	18,900	13,300
Never Smokers	11,000	2,900	2,100
Male	95,400	12,500	8,800
Ever Smokers	90,600	11,300	7,900
Never Smokers	4,800	1,200	900
Female	62,000	9,300	6,600
Ever Smokers	55,800	7,600	5,400
Never Smokers	6,200	1,700	1,200

* From the BEIR VI Report.

tude higher than average indoor radon-daughter exposures, although there is some overlap.

In addition to the disparity in dose levels, other factors complicate the application of the uranium-miner experience to an assessment of lung-cancer risk from radon at the relatively low levels in the general population. There are differences between inhaled particle sizes, equilibrium factors, and unattached fractions. There are differences between the breathing rates and physiological characteristics of the male miners and members of all ages and the two sexes in the public. Cigarette smoking is the greatest cause of lung cancer in the world, and most uranium miners were smokers. Synergistic effects occur with the two carcinogens, radon daughters and cigarette smoke.

For estimation of the risk to the general public due to radon, BEIR VI focused on that fraction of the total lung-cancer burden that could presumably be prevented if all radon population exposures were reduced to the background levels of ambient outside air. Compared with outdoors, indoor levels can be considerably higher. Table 13.5 shows an analysis of lung-cancer deaths in the United States for the year 1995, based on data in the BEIR VI Report. The total number of 157,400 deaths, given in the second column, is divided between persons who ever smoked and those who never smoked. A further subdivision is made for males and females. Most of the cases occurred in smokers. Under assumptions used in two preferred risk models, which deal differently with the influence of cigarette smoking, the number of deaths attributable to indoor residential radon daughters was estimated. Model 1 projected 21,800 and Model 2, 15,400 deaths due to residential radon exposures. Thus, the estimates of the two models in Table 13.5 imply that about 1 in 7, or 1 in 10, of all lung-cancer deaths in the U.S. are due indoor residential radon. The BEIR Committee suggested that the number could range from 3,000 to 30,000. As a public-health problem, this assessment clearly identifies indoor radon as the second leading cause of lung cancer after cigarette smoking.

Accidents

Accidents provide yet another source of information on radiation effects on man, particularly acute effects at high doses. Several fatal accidents have happened with critical assemblies. Serious accidents have occurred with particle accelerators. A larger number of accidental or unknowingly high exposures have resulted from handling radiation devices (X-ray machines and sealed sources) and radioisotopes. Other examples can be cited. In March 1954, high-level fallout from the BRAVO nuclear weapons test reached several Bikini atolls, resulting in substantial doses to some weather-station personnel and Marshallese natives, who were then evacuated. Thyroid abnormalities, including cancer, developed subsequently. In addition, a Japanese fishing vessel *(The Lucky Dragon)* received a large amount of (visible) fallout. The twenty-three men on board suffered massive skin burns and other damage, which could have been lessened considerably by simply rinsing the skin.

On April 26, 2006 the world marked the 20th anniversary of the Chernobyl power-reactor accident in Ukraine, just south of the border with Belarus. It was the most severe accident ever in the nuclear industry. Some 50 persons died within days or weeks, some from the consequences of radiation exposure. (By comparison, the highest individual dose from the 1979 accident at Three Mile Island in the United States was less than 1 mSv.[4]) Enormous quantities of radioactive material were spewed into the atmosphere over a period of days, spreading a cloud of radionuclides over Europe. The resulting contamination of large areas in Belarus, Ukraine, and the Russian Federation led to the relocation of several hundred thousand individuals.

The accident occurred during a low-power test as the result of procedural violations, failure to understand the reactor's behavior, and poor communication between the responsible parties on site. The reactor was being operated with too few control rods, some safety systems shut off, and the emergency cooling system disabled. Even at low power, excess steam pockets (voids) could form in the light-water coolant, thus reducing neutron absorption and increasing the power output, resulting in more voids (positive void coefficient). Reactor control could be quickly lost, as apparently happened.

The consequences were devastating. The acute radiation syndrome (Section 13.8) was confirmed in more than 100 plant employees and first responders, some resulting in death. Severe skin burns from beta radiation occurred. Measurements of blood ^{24}Na activation indicated that neutrons contributed little to individual doses. Epidemiologic studies have been carried out and are continuing. There is a registry of medical and dosimetric information on hundreds of thousands of individuals. Significant data showing health effects in terms of increased incidence of leukemia and thyroid cancer are well documented. Elevated incidence of thyroid cancer in

4 NCRP Report No. 93, *Ionizing Radiation Exposure of the Population of the United States*, p. 28, National Council on Radiation Protection and Measurements, Bethesda, MD (1987).

children and adolescents is a major effect from the Chernobyl accident. Figure 13.7 shows an example of findings from one study.

Additional information on what has been learned from radiation accidents can be found in several of the references listed in Section 13.15 and on the World Wide Web. Experience with the medical and logistic management of radiation accidents also has important lessons for dealing with potential terrorist attacks that might involve radiation.[5)]

13.8
The Acute Radiation Syndrome

If a person receives a single, large, short-term, whole-body dose of radiation, a number of vital tissues and organs are damaged simultaneously. Radiosensitive cells become depleted because their reproduction is impeded. The effects and their severity will depend on the dose and the particular conditions of the exposure. Also, specific responses can be expected to differ from person to person. The complex of clinical symptoms that develop in an individual plus the results of laboratory and bioassay findings are known, collectively, as the acute radiation syndrome.

The acute radiation syndrome can be characterized by four sequential stages. In the initial, or prodromal, period, which lasts until about 48 h after the exposure, an individual is apt to feel tired and nauseous, with loss of appetite (anorexia) and sweating. The remission of these symptoms marks the beginning of the second, or latent, stage. This period, from about 48 h to 2 or 3 wk postexposure, is characterized by a general feeling of well being. Then in the third, or manifest illness, stage, which lasts until 6 or 8 wk postexposure, a number of symptoms develop within a short time. Damage to the radiosensitive hematologic system will be evident through hemorrhaging and infection. At high doses, gastrointestinal symptoms will occur. Other symptoms include fever, loss of hair (epilation), lethargy, and disturbances in perception. If the individual survives, then a fourth, or recovery, stage lasts several additional weeks or months.

Depending on the dose received, the acute radiation syndrome can appear in a mild to very severe form. Table 13.6 summarizes typical expectations for different doses of gamma radiation, which, because of its penetrating power, gives an approximately uniform whole-body dose.

An acute, whole-body, gamma-ray dose of about 4 Gy without treatment would probably be fatal to about 50% of the persons exposed. This dose is known as the LD50—that is, the dose that is lethal to 50% of a population. More specifically, it is also sometimes called the LD50/30, indicating that the fatalities occur within 30 days.

5 See the Proceedings of the 40th Annual Meeting of the NCRP: Advances in Consequence Management for Radiological Terrorism Events, *Health Phys.* **89**, 415–588 (2005).

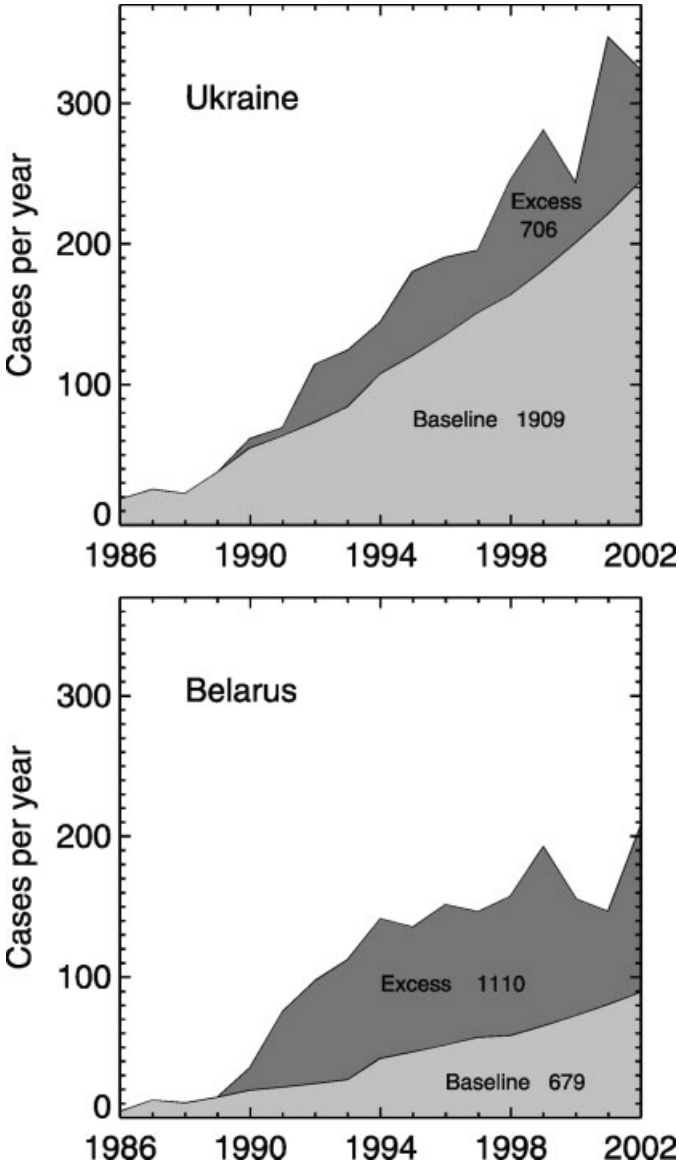

Fig. 13.7 Annual number of thyroid cancer cases among the birth-year cohorts 1968 to 1985 in Ukraine and Belarus. The total number of observed cases is split into spontaneous (baseline) and excess cases due to ^{131}I exposures after the Chernobyl accident. The baseline number increases with calendar year, because of aging of the cohort (i.e., the baseline increases with age) and because of intensified surveillance of the thyroid in the aftermath of the accident. After P. Jacob, T. I. Bogdanova, E. Buglova, M. Chepurniy, Y. Demidchik, Y. Gavrilin, J. Kenigsberg, J. Kruk, C. Schotola, S. Shinkarev, M. D. Tronko, and S. Vavilov, "Thyroid Cancer among Ukranians and Belarusians who were Children or Adolescents at the Time of the Chernobyl Accident," *J. Radiol. Ptcn.* **26**, 51–67 (2006). (Courtesy Peter Jacob, GSF National Research Center, Neuherberg, Germany.)

Table 13.6 Acute Radiation Syndrome for Gamma Radiation

Dose (Gy)	Symptoms	Remarks
0–0.25	None	No clinically significant effects.
0.25–1	Mostly none. A few persons may exhibit mild prodromal symptoms, such as nausea and anorexia.	Bone marrow damaged; decrease in red and white blood-cell counts and platelet count. Lymph nodes and spleen injured; lymphocyte count decreases.
1–3	Mild to severe nausea, malaise, anorexia, infection.	Hematologic damage more severe. Recovery probable, though not assured.
3–6	Severe effects as above, plus hemorrhaging, infection, diarrhea, epilation, temporary sterility.	Fatalities will occur in the range 3.5 Gy without treatment.
More than 6	Above symptoms plus impairment of central nervous system; incapacitation at doses above ~10 Gy.	Death expected.

13.9 Delayed Somatic Effects

As indicated in Table 13.1, some biological effects of radiation, administered either acutely or over an extended period, may take a long time to develop and become evident. Such changes are called delayed, or late, somatic effects. In contrast to genetic effects, which are manifested in the offspring of an irradiated parent or parents, late somatic effects occur in the exposed individual. Documentation of late somatic effects due to radiation and estimations of their risks, especially at low doses, are complicated by the fact that the same effects occur spontaneously. The human data on which we focus in this section are supported and expanded by extensive animal experiments.

Cancer

The risk of getting cancer from radiation depends on many factors, such as the dose and how it is administered over time; the site and particular type of cancer; and a person's age, sex, and genetic background. Additional factors, such as exposure to other carcinogens and promoters, are also important. Cancer causes almost 20% of all deaths in the United States. The relatively small contribution made by low levels of radiation to this large total is not statistically evident in epidemiological studies. In addition, radiogenic cancers are not distinguishable from other cancers. As stated in the BEIR VII Report, "At doses less than 40 times the aver-

Table 13.7 Lifetime Risk for Incidence and Mortality for All Solid Cancers and for Leukemia from a Dose of 0.1 Gy to 100,000 Persons in a Population Similar to that of the U.S.*

	All Solid Cancers		Leukemia	
	Male	**Female**	**Male**	**Female**
Excess cases	800	1,300	100	70
Number cases without dose	45,500	36,900	830	590
Excess deaths	410	610	70	50
Number deaths without dose	22,100	17,500	710	530

* Adapted from BEIR VII Report (see references, Section 13.15).

age yearly background exposure (100 mSv), statistical limitations make it difficult to evaluate cancer risk in humans." Thus, cancer risk at low doses can at present only be estimated by extrapolation from human data at high doses, where excess incidence is statistically detectable.

Probably the most reliable risk estimates for cancer due to low-LET radiation are those for leukemia and for the thyroid and breast. The minimum latent period of about 2 y for leukemia is shorter than that for solid cancers. Excess incidence of leukemia peaked in the Japanese survivor population around 10 y post-exposure and decreased markedly by about 25 y. These observations are consistent with leukemia experience from other sources, such as patients treated for ankylosing spondylitis and for carcinoma of the uterine cervix. Solid tumors induced by radiation require considerably longer to develop than leukemia. Radiogenic cancers can occur at many sites in the body. We mentioned bone cancers in the radium-dial painters and lung cancers in the uranium miners. The BEIR VII Report provides extensive, detailed information on a wide variety of radiogenic cancers.

The BEIR VII Committee undertook the task of developing models for estimating risks between exposure to low doses of low-LET radiation and adverse health effects. They derived models for both cancer incidence and cancer mortality, allowing for dependence on sex, age at exposure, and time since exposure. Estimates are presented for all solid cancers, leukemia, and a number of site-specific cancers. Special assumptions (e.g., a DDREF) were applied when estimates in lifetime risks for the U.S. population were made from data in the Life Span Study. As an example, Table 13.7 gives a summary from the BEIR VII Report for lifetime risks for all solid cancers and for leukemia. The Committee considered a *linear-no-threshold* model as the most reasonable for describing solid cancers and a *linear-quadratic* model for leukemia (cf., Fig. 13.5). The first line in the table shows the excess number of cancer cases for males and females that would be expected if a population of 100,000 persons, having an age distribution similar to that of the U.S., were to receive a dose of 0.1 Gy of low-LET radiation. The number of cases in the absence of this exposure is shown in the next line. The third and fourth lines display the corresponding information for cancer deaths.

Life Shortening

Numerous experiments have been carried out in which animals are given sublethal doses of whole-body radiation at various levels. The animals apparently recover, but are subsequently observed to die sooner than controls. This decreased life expectancy was originally described as nonspecific radiation life shortening or as radiation aging. More thorough studies of the effects of low doses of radiation, particularly with careful autopsy examinations, showed that the life shortening due to radiation in animal populations can be attributed to an excess of neoplasia rather than a generally earlier onset of all causes of death. The preponderance of evidence indicates that radiation life shortening at low doses is highly specific, being primarily the result of an increased incidence of leukemia and cancer.

Some investigations have reported a longer average life expectancy in animals exposed to low levels of whole-body radiation than in unexposed controls. Such reports are offered by some as evidence of *radiation hormesis*—that is, the beneficial effect of small doses of radiation. Radiation hormesis has also been extensively investigated in plants, insects, algae, and other systems. As with other low-dose studies of biological effects of radiation, one deals with relatively small effects in a large statistical background of naturally occurring endpoints. Theoretical grounds can be offered in support of low-level radiation hormesis—e.g., stimulation of DNA repair mechanisms that reduce both radiation-induced and spontaneous damage. Evidence for hormesis has been reviewed by the BEIR VII Committee and other bodies. (See references in Section 13.15.) The BEIR VII Report summarizes its judgement in stating, "... the assumption that any stimulatory hormetic effects from low doses of ionizing radiation will have a significant health benefit to humans that exceeds potential detrimental effects from the radiation exposure is unwarranted at this time."

Cataracts

The biological effects discussed thus far in this section are stochastic. In contrast, a radiogenic cataract is a deterministic effect. There is a practical threshold dose below which cataracts are not produced; and their severity, when they occur, is related to the magnitude of the dose and the time over which it is administered. A cataract is an opacification of the lens of the eye. The threshold for ophthalmologically detectable lens opacification, as observed in patients treated with X rays to the eye, ranges from about 2 Gy for a single exposure to more than 5 Gy for multiple exposures given over several weeks. This level is also consistent with data from Hiroshima and Nagasaki. The threshold for neutrons appears to be lower than for gamma rays. The latent period for radiogenic cataracts is several years, depending on the dose and its fractionation.

Among the biological effects of radiation, a unique feature of a radiogenic cataract is that it can usually be distinguished from other cataracts. The site of the initial detectable opacity on the posterior pole of the lens and its subsequent developmental stages are specific to many radiation cataracts.

13.10
Irradiation of Mammalian Embryo and Fetus

Rapidly dividing cells and tissues in which cells are continually being replaced are among the most radiosensitive: the gonads, gastrointestinal tract, blood-forming organs, lymphatic system, and skin. The developing embryo and fetus, in particular, are highly vulnerable to adverse radiogenic effects, which have been documented in man and in experimental animals.

The principal effects of *in-utero* irradiation are prenatal death, growth retardation, and congenital malformations (teratogenesis). The degree of such effects varies markedly with the stage of development at the time of irradiation. Three such stages can be identified: (1) preimplantation, the time between fertilization of the egg and its implantation in the uterine lining; (2) maximum organogenesis, the time during maximal formation of new organs; and (3) fetal, the final stage, with growth of preformed organs and minimum organogenesis. In humans, these periods are approximately, 0 to 9 d, 10 d to 6 wk, and 6 wk to term.

The unborn is considerably more sensitive to being killed when in the preimplantation stage than later. However, growth retardation and teratogenesis are not generally found as a result of exposure during this stage. Presumably, changes before implantation that predispose the multicellular embryo to such later effects also induce its death. The unborn is most susceptible to teratogenesis when irradiated during the stage of maximum organogenesis. Figure 13.8 shows an example of deformities in a calf whose mother was given 4 Gy of whole-body gamma radiation on the 32nd day after its conception. Calves irradiated similarly, but two additional days after conception, showed little or no damage of this kind. Irradiation during the fetal, or final, stage also produces the greatest degree of permanent growth retardation.

Other types of biological damage have been seen in animals irradiated *in utero* at high doses. However, many of these effects do not appear to occur to the same degree in man, with the exception of damage to the central nervous system. The latter provides, in fact, the most definitive data for an effect of prenatal irradiation in man. The increased prevalence of mental retardation and of microcephaly (small head size), for example, have been documented among the prenatally exposed Japanese survivors.

As described in the next chapter (Section 14.6), special restrictions are recommended by the ICRP and NCRP for the occupational exposure of women of childbearing age and, especially, pregnant women.

13.11
Genetic Effects

Mueller discovered the mutagenic property of ionizing radiation in 1927. Like a number of chemical substances, radiation can alter the genetic information con-

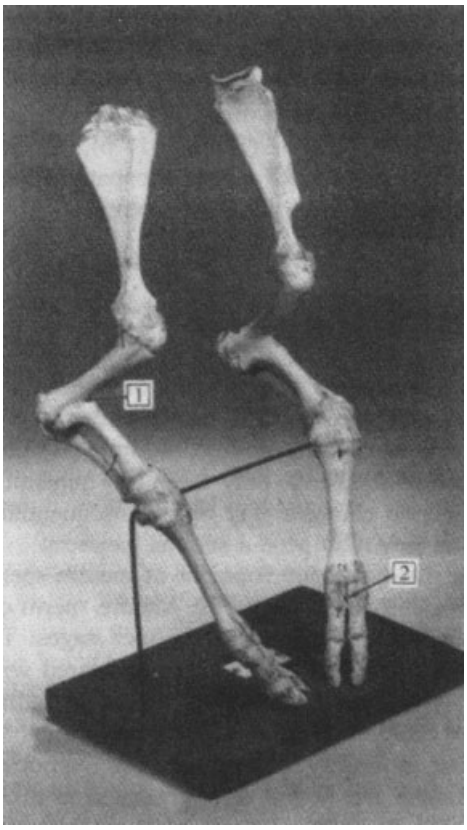

Fig. 13.8 Effects of prenatal irradiation (4 Gy, whole-body gamma, on 32d day of gestation) on anatomical development of a calf are seen in severe deformities of the forelimbs at birth: (1) bony ankylosis of the humero-radial joints and (2) deformities of the phalanges. In addition, the posterior surfaces of the limbs are turned inward. Such effects are dose- and time-specific. Other fetal calves irradiated two days later suffered only minor damage to the phalanges. (Courtesy G. R. Eisele and W. W. Burr, Jr., Medical and Health Sciences Division, Oak Ridge Associated Universities, Oak Ridge, TN.)

tained in a germ cell or zygote (fertilized ovum). Although mutations can be produced in any cell of the body, only these can transmit the alterations to future generations. Genetic changes may be inconsequential to an individual of a later generation or they may pose a serious handicap.

In the adult human male, the development of mature sperm from the spermatogonial stem cells takes about 10 weeks. Mature sperm cells are produced continually, having passed through several distinct stages. The postspermatogonal cells are relatively resistant to radiation, compared with the stem cells. Thus, an adult male who receives a moderate dose of radiation will not experience an immediate decrease in fertility. However, as his mature sperm cells are depleted, a decrease in fertility, or even sterility, will occur. Depending on the magnitude of the dose and how it is fractionated in time, sterility can be temporary or permanent in males.

The 1990 BEIR V Report (see Section 13.15) states than an acute X-ray dose of 0.15 Gy to the human testes interrupts spermatozoa production to the extent that temporary infertility results. An X-ray dose of 3 to 5 Gy, either acute of fractionated over several weeks, can cause permanent sterility.

In the adult human female, all germ cells are present as ooctyes soon after birth. There are no (oogonial) stem cells, and there is no cell division. The BEIR V Report states than an acute dose of 0.65 to 1.5 Gy to the human ovary impairs fertility temporarily. Fractionation of the dose to the ovaries over several weeks considerably increases the tolerance to radiation. The threshold for permanent sterility in the adult human female for X irradiation of the ovaries is in the range from 2.5 to 6 Gy for acute exposure and is about 6 Gy for protracted exposure.

Every normal cell in the human has 46 paired chromosomes, half derived from the father and half from the mother. Each chromosome contains genes that code for functional characteristics or traits of an individual. The genes, which are segments of deoxyribonucleic acid (DNA), are ordered in linear fashion along a chromosome. The DNA itself is a macromolecule whose structure is a linear array of four varieties of bases, hydrogen bonded in pairs into a double-helical structure. The particular sequence of bases in the DNA encodes the entire genetic information for an individual. The human genome contains about 6×10^9 base pairs and perhaps 50,000 to 100,000 genes.

Mutations occur naturally and spontaneously among living things. Various estimates indicate that no more than about 5% of all natural mutations in man are ascribable to background radiation. Radicals produced by metabolism, random thermal agitation, chemicals, and drugs, for example, contribute more.

A useful, quantitative benchmark for characterizoing radiation-induced mutation rates is the *doubling dose*. It is defined as the amount of radiation that produces in a generation as many mutations as arise spontaneously. For low-dose-rate, low-LET radiation, the BEIR V Report estimated the doubling dose for mice to be about 1 Gy for various genetic endpoints. It noted that this level is not inconsistent with what might be inferred for man from the atomic-bomb survivors. The BEIR VII Report reviews and discusses doubling-dose estimates, which have been almost exclusively based on both spontaneous and radiation induced rates in mice. The Committee concludes that extrapolation of the doubling dose based on mice for risk estimation in humans should be made with the *human* spontaneous rate. It reports a revised estimate of 0.82 ± 0.29 Gy, and suggests retaining the value 1 Gy for the doubling dose as an average rate for mutations.

Radiation-induced genetic changes can result from gene mutations and from chromosome alterations. A gene mutation occurs when the DNA is altered, even by a loss or substitution of a single base. The mutation is called a point mutation when there is a change at a single gene locus. Radiation can also cause breakage and other damage to chromosomes. Some mutations involve a deletion of a portion of a chromosome. Broken chromosomes can rejoin in various ways, introducing errors into the normal arrangement. Figure 13.9 shows two examples of chromosome aberrations induced in human lymphocytes by radiation. Chromosome aberrations

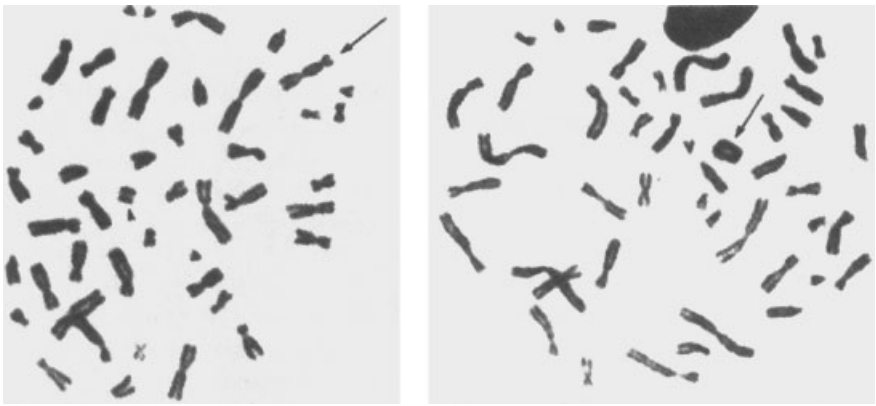

Fig. 13.9 Radiation-induced chromosome aberrations in human lymphocytes. Left: chromosome-type dicentric (↙) and accompanying acentric fragment (►). Right: chromosome-type centric ring (↙). The accompanying acentric fragment is not included in the metaphase spread. (Courtesy H. E. Luippold and R. J. Preston, Oak Ridge National Laboratory, operated by Martin Marietta Energy Systems, Inc., for the Department of Energy.)

occur in somatic cells. Figure 13.10 illustrates genetic effects of radiation in the fruit fly.

The most extensive studies of the genetic effects of radiation on mammals have been carried out with mice by W. L. Russell and L. B. Russell. Using literally millions of mice, they investigated specific locus mutation rates under a variety of conditions of dose, dose rate, and dose fractionation. When compared with the limited amount of data available for humans, it appears that the data for genetic effects in the mouse can be applied to man with some degree of confidence. These data play an important part in assessing the genetic risk and impact on man associated with the recommended radiation limits to be discussed in the next chapter. We mentioned earlier the doubling dose for mutations in mice, which was established by the Russells' work. They also measured substantial dose-rate effects on mutations in the mouse. Protraction of a given dose over time results in fewer mutations than when the same dose is given acutely, indicating that repair processes come into play. Males are much more sensitive than females for the induction of genetic damage by radiation. The latter show little, if any, increased mutation frequency at low dose rates, even for total accumulated doses of several Gy. Also, mutagenic effects are lowered when mating is delayed after irradiation.

Radiation does not induce any kinds of mutations that do not occur naturally. As with other biological endpoints, genetic effects due to radiation are added to an existing spontaneous pool, thus obscuring their quantitative assessment. An additional complication arises, because genetic effects are expressed only in the immediate or later offspring of the irradiated individuals.

Fig. 13.10 Top: normal Drosophila male. Bottom: Drosophila male with four wings resulting from one spontaneous and two X-ray induced mutations. [Source: E. B. Lewis, California Institute of Technology. Reprinted with permission from J. Marx, "Genes that Control Development," *Science* **213**, 1485–1488 (1981). Copyright 1981 by the American Association for the Advancement of Science.]

13.12
Radiation Biology

Radiation biology is rapidly advancing our knowledge about the biological effects of radiation. It is beyond the scope of this book to attempt any meaningful review of the varied research being carried out in this exciting field. Studies are directed at discovering and understanding fundamental mechanisms of molecular and cellular responses to radiation.

The complex types of DNA damage produced by radiation can be broadly classified as single-strand breaks, double-strand breaks, and base damages. These structural changes and errors in their repair can lead to gene mutations and chromosomal alterations. A great deal is understood about the molecular details of DNA damage repair and misrepair and its relation to potential tumor induction and other adverse health effects. How a cell operates to deter or prevent the transmission of genetic damage to its progeny is still an unfolding story. Intricate controls exercised by molecular checkpoint genes at specific stages of the cell reproductive cycle appear to recognize and react to the management and repair of damaged DNA.

In order to cause genetic alterations in a cell, it has generally been assumed (or taken for granted) that the cell nucleus must be traversed by a charged-particle track. Research has revealed, however, that nearby cells—called *bystanders*—can also sustain genetic damage, even though no tracks pass through them and hence they presumably receive little or no radiation dose. Studies have been conducted at very low flunece and also with micro-beams directed at individual cells in a target. Mechanisms responsible for producing bystander effects are under investigation. Evidence appears to indicate that mutations in bystander cells with some systems are induced by a different mechanism than those in the directly traversed cells.

Genomic instability, which describes the increased rate of accumulation of new genetic changes after irradiation, is observed in some of the progeny of both directly irradiated and bystander cells. The underlying mechanisms for the induction and persistence of genomic instability, which is particularly relevant to tumor development, are poorly understood at present.

In some systems, a small dose of radiation (e.g., several mGy) triggers a cellular response that protects the cells from a large dose of the radiation given subsequently. This phenomenon, which is not universal in all test systems, is called the *adaptive response*. The bacterium *Escherichia coli*, for example, shows a definite adaptive response to oxidative stress. Exposure to a low dose of radiation induces cellular transcription reprogramming. A result is the increased expression of entities that inactivate reactive oxygen species and that repair oxidative DNA damage. For a finite length of time after the initial small priming dose, the bacterial cells are more resistant to a large dose of the radiation than they would be otherwise. Human cells do not show such an adaptive response to oxidative damage. One should note that adaptive response is not the same as hormesis, which ascribes an overall benefit from a small dose of radiation dose.

As more is learned in radiation biology, greater confidence can be placed in the assessment of risk estimates for exposure of persons to ionizing radiation, particularly at low doses. Understanding the basic molecular mechanisms of radiation damage in cells will greatly facilitate the task. We turn next to the subject of dose–response relationships, which underlie radiation-protection regulations in use today.

13.13 Dose–Response Relationships

Biological effects of radiation can be quantitatively described in terms of dose–response relationships, that is, the incidence or severity of a given effect, expressed as a function of dose. These relationships are conveniently represented by plotting a dose–response curve, such as that shown in Fig. 13.11. The ordinate gives the observed degree of some biological effect under consideration (e.g., the incidence of certain cancers in animals per 100,000 population per year) at the dose level given by the abscissa. The circles show data points with error bars that represent a specified confidence level (e.g., 90%). At zero dose, one typically has a natural, or spontaneous, level of incidence, which is known from a large population of unexposed individuals. Often the numbers of individuals exposed at higher dose levels are relatively small, and so the error bars there are large. As a result, although the trend of increasing incidence with dose may be clearly evident, there is no unique dose–response curve that describes the data. In the figure, a solid straight line, consistent with the observations, has been drawn at high doses. The line is constructed in such a way that it intersects the ordinate at the level of natural incidence when a linear extension (dashed curve A) to zero dose is made. In this case, we say that a linear dose–response curve, extrapolated down to zero dose, is used to represent the effect.

Curves with other shapes can usually be drawn through biological dose–effect data. An example of this kind of response is found for leukemia in the atomic-bomb survivors, shown by the inset in Fig. 13.5. Also, extrapolations to low doses can be made in a number of ways. Sometimes there are theoretical reasons for assuming a particular dose dependence, particularly at low doses. The dashed curve B in Fig. 13.11 shows a nonlinear dependence. Both curves A and B imply that there is always some increased incidence of the effect due to radiation, no matter how small the dose. In contrast, the extrapolation shown by the curve C implies that there is a threshold of about 0.75 Gy for inducing the effect.

For many endpoints of carcinogenesis, mutagenesis, and other effects, dose–response functions at low doses and low dose rates can be analyzed in the following way, contrasting high- and low-LET radiations. With low doses of high-LET radiation, the effect is presumably due to individual charged-particle tracks: their spatial density is small, and there is a negligible overlap of different tracks. Since the density of tracks is proportional to the dose, the incidence $E(D)$ (above controls) should also be proportional to the dose D at low doses. This general behavior of the dose

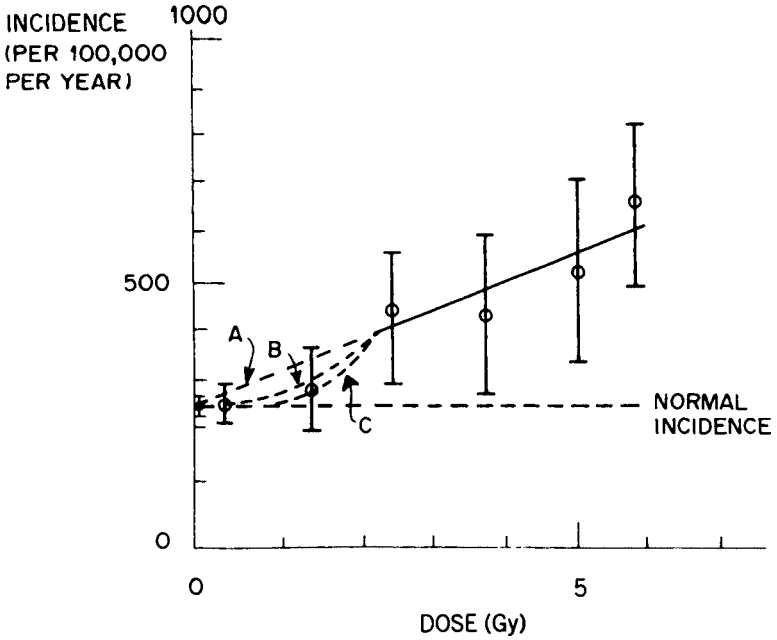

Fig. 13.11 Example of a dose–response curve, showing the incidence of an effect (e.g., certain cancers per 100,000 population per year) as a function of dose. Circles show measured values with associated error bars. Solid line at high doses is drawn to extrapolate linearly (dashed curve A) to the level of normal incidence at zero dose. Dashed curve B shows a nonlinear extrapolation to zero dose. Dashed curve C corresponds to having a threshold of about 0.75 Gy.

response at low doses for high-LET radiation is shown in Fig. 13.12 by the curve H (which may even begin to decrease in slope at high doses).

For low-LET radiation, dose–response curves in many cases appear to bend upward as the dose increases at low doses and low dose rates, as indicated by the curve L_1 in Fig. 13.12. Such behavior is consistent with a quadratic dependence of the magnitude $E(D)$ of the effect as a function of the dose D:

$$E(D) = \alpha D + \beta D^2. \tag{13.13}$$

Here α and β are constants whose values depend on the biological effect under study, the type of radiation, the dose rate, and other factors. This mathematical form of response, which is commonly referred to as "linear-quadratic" (a misnomer), has a theoretical basis in association with a requirement that *two* interacting lesions are needed to produce the biological damage observed. (It dates back to the 1930s, when it was employed to describe the dose response for some chromosome aberrations, which result from interactions between breaks in two separate chromatids.) As with high-LET radiation, the effect at very low doses must be due to individual tracks. As the dose is increased, the chance for two tracks to overlap soon becomes appreciable at low LET. The response for two-track events should increase as the square of the dose. The initial linear component of the dose–response

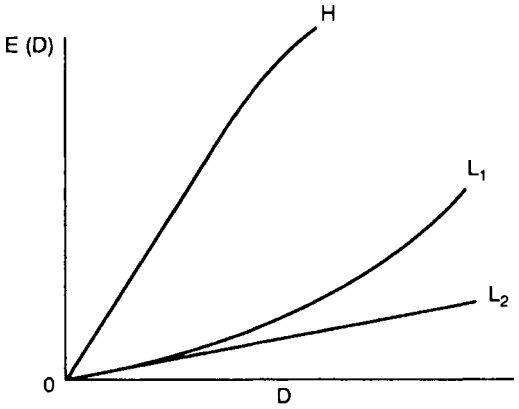

Fig. 13.12 Schematic representation of dose–response function $E(D)$ at low doses D for high-LET (curve H) and low-LET (curve L_1) radiations. L_2 is the extension of the linear beginning of L_1.

function for the low-LET radiation is shown by the curve L_2 in Fig. 13.12. To deal with stochastic effects of radiation, the setting of occupational dose limits has been done in a manner consistent with L_2. This *linear-nonthreshold* (*LNT*) dose–response model will be discussed in the next chapter.

Linear-quadratic dose–response relationships are often used to analyze and fit various biological data. However, interpretations other than one- and two-track events can be made to explain their shape. It can be argued, for example, that only single-track damage occurs and that biological repair comes into play, but saturates at high doses. Such a model predicts an upward bend in the dose–response curve with increasing dose.

Another important kind of dose–response relationship is illustrated by the survival of cells exposed to different doses of radiation. The endpoint studied is cell inactivation, or killing, in the sense of cellular reproductive death, or loss of a cell's ability to proliferate indefinitely. Large cell populations can be irradiated and then diluted and tested for colony formation. Cell survival can be measured over three and sometimes four orders of magnitude. It provides a clear, quantitative example of a cause-and-effect relationship for the biological effects of radiation. We next consider cell survival and use it as an example for dose–response modeling.

Cell inactivation is conveniently represented by plotting the natural logarithm of the surviving fraction of irradiated cells as a function of the dose they receive. A linear semilog survival curve, such as that shown in Fig. 13.13, implies exponential survival of the form

$$\frac{S}{S_0} = \mathrm{e}^{-D/D_0}. \tag{13.14}$$

Here S is the number of surviving cells at dose D, S_0 is the original number of cells irradiated, and D_0 is the negative reciprocal of the slope of the curve in Fig. 13.13. Analogous to the reciprocals of λ in Eq. (4.22) and μ in Eq. (8.43), it is called the

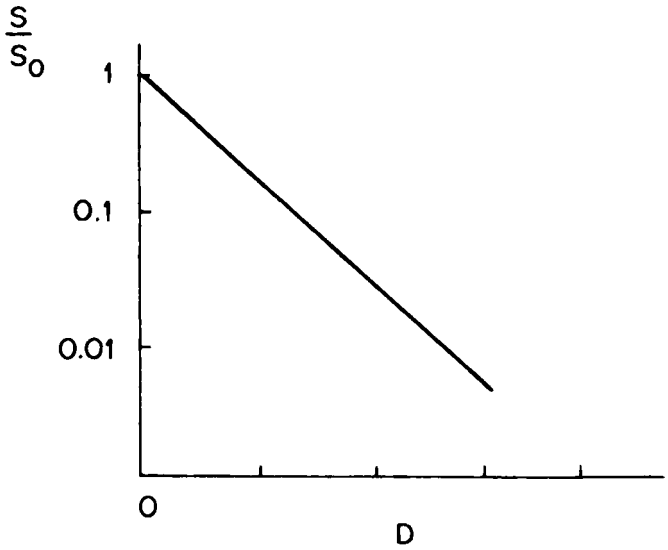

Fig. 13.13 Semilogarithmic plot of surviving fraction S/S_0 as a function of dose D, showing exponential survival characterized by straight line.

mean lethal dose; D_0 is therefore the average dose absorbed by each cell before it is killed. The surviving fraction when $D = D_0$ is, from Eq. (13.14),

$$\frac{S}{S_0} = e^{-1} = 0.37. \tag{13.15}$$

For this reason, D_0 is also called the "D-37" dose.

Exponential behavior can be accounted for by a "single-target," "single-hit" model of cell survival. We consider a sample of S_0 identical cells and postulate that each cell has a single target of cross section σ. We postulate further that whenever radiation produces an event, or "hit," in a cellular target, then that cell is inactivated and does not survive. The biological target itself and the actual physical event that is called a hit need not be specified explicitly. On the other hand, one is free to associate the target and its size with cellular DNA or other components and a hit with an energy-loss event in the target, such as a neutron collision or traversal by a charged particle. When the sample of cells is exposed uniformly to radiation with fluence φ, then the total number of hits in cellular targets is $\varphi S_0 \sigma$. Dividing by the number of cells S_0 gives the average number of hits per target in the cellular population: $\bar{k} = \varphi\sigma$. The distribution of the number of hits per target in the population is Poisson (Problem 27). The probability of there being exactly k hits in the target of a given cell is therefore $P_k = \bar{k}^k e^{-k}/k!$. The probability that a given cell survives the irradiation is given by the probability that its target has no hits: $P_0 = e^{-\bar{k}} = e^{-\varphi\sigma}$.

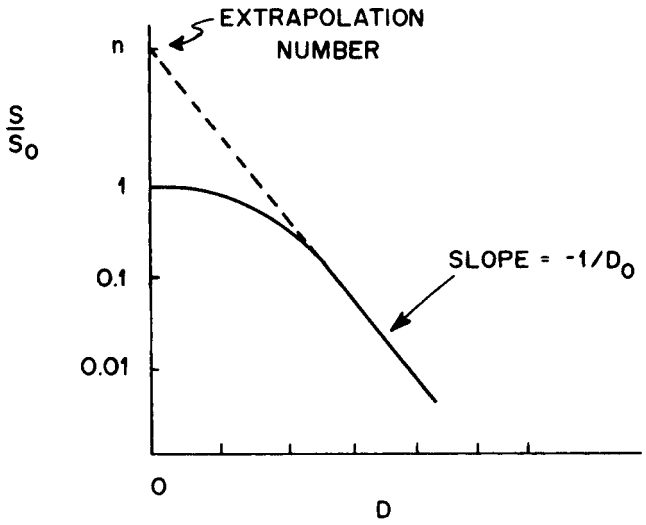

Fig. 13.14 Semilogarithmic plot of multitarget, single-hit survival.

Thus, the single-target, single-hit model predicts exponential cell survival. Since $P_0 = S/S_0$, we can extend Eq. (13.14) by writing

$$\frac{S}{S_0} = e^{-D/D_0} = e^{-\varphi\sigma}. \tag{13.16}$$

In terms of the model, the inactivation cross section gives the slope of the survival curve on the semilog plot in Fig. 13.13.

A model that yields a survival curve with a different shape is multitarget, single-hit. In this case, n identical targets with cross section σ are ascribed to a cell; and all targets in a given cell must be hit at least once in order to inactivate it. As before, we apply Poisson statistics with $\varphi\sigma = D/D_0$ denoting the average number of hits in a given cell target with fluence φ. The probability that a given target in a cell is hit (one or more times) is equal to one minus the probability that it has not been hit: $1 - e^{-D/D_0}$. The probability that all n targets in a cell are hit is $(1 - e^{-D/D_0})^n$, in which case the cell is inactivated. The survival probability for the cell is therefore

$$\frac{S}{S_0} = 1 - (1 - e^{-D/D_0})^n. \tag{13.17}$$

When $n = 1$, this equation reduces to the single-target, single-hit result. For $n > 1$ the survival curve has the shape shown in Fig. 13.14. There is a shoulder that begins with zero slope at zero dose, reflecting the fact that more than one target must be hit in a cell to inactivate it. As the dose increases, cells accumulate additional struck targets; and so the slope steadily increases. At sufficiently high doses, surviving cells are unlikely to have more than one remaining unhit target. Their response then takes on the characteristics of single-target, single-hit survival, and additional dose produces an exponential decrease with slope $-1/D_0$ on the semilog plot. When

D is large, e^{-D/D_0} is small, and one can use the binomial expansion[6] to write, in place of Eq. (13.17),

$$\frac{S}{S_0} \cong 1 - (1 - ne^{-D/D_0}) = ne^{-D/D_0}. \tag{13.18}$$

The straight line represented by this equation on a semilog plot intercepts the ordinate ($D = 0$) at the value $S/S_0 = n$, which is called the extrapolation number. As shown in Fig. 13.14, the number of cellular targets n is thus obtained by extrapolating the linear portion of the survival curve back to zero dose.

Many experiments with mammalian cells yield survival curves with shoulders. However, literal interpretation of such data in terms of the elements of a multitarget, single-hit model is not necessarily warranted. Cells in a population are not usually identical. Some might be in different stages of the cell cycle, with different sensitivity to radiation. Repair of initial radiation damage can also lead to the existence of a shoulder on a survival curve.

Still other models of cell survival have been investigated. The multitarget, single-hit model can be modified by postulating that only any $m < n$ of the cellular targets need to be hit in order to produce inactivation. Single-target, multihit models have been proposed, in which more than one hit in a single cellular target is needed for killing. In addition to these target models, other theories of cell survival are based on different concepts.

13.14 Factors Affecting Dose Response

Relative Biological Effectiveness

Generally, dose–response curves depend on the type of radiation used and on the biological endpoint studied. As a rule, radiation of high LET is more effective biologically than radiation of low LET. Different radiations can be contrasted in terms of their relative biological effectiveness (RBE) compared with X rays. If a dose D of a given type of radiation produces a specific biological endpoint, then RBE is defined as the ratio

$$\text{RBE} = \frac{D_x}{D}, \tag{13.19}$$

where D_x is the X-ray dose needed under the same conditions to produce the same endpoint. As an example, irradiation of *Tradescantia* (spiderwort) produces in stamen hairs pink mutant events that can be counted and scored quantitatively. In experiments with 680-keV neutrons and 250-kVp X rays, it is observed that 0.030 pink events per hair (minus control) are produced by a dose of 16.5 mGy with the

6 For small x, $(1 - x)^n \cong 1 - nx$.

neutrons and 270 mGy with the X rays. It follows that the RBE for this specific effect is $270/16.5 = 16.4$.[7)]

Figure 13.15 shows examples of dose–response curves for irradiation of Sprague-Dawley rats with X rays and with 430-keV neutrons.[8)] Groups of rats at age 60 d were given X-ray doses of 0.28, 0.56, and 0.85 Gy and neutron doses of 0.001, 0.004, 0.016, and 0.064 Gy. The straight lines fit the measured data, indicated by the dots in the figure. RBE values at two levels of response for each of the four effects are shown for illustration. One sees that the RBE is different numerically for the four effects and that it also depends on the level of the effect. Its values span the range between 13 and 190 and beyond. As found here and in many experiments, RBE values are largest for small levels of effect. Generally, relative biological effectiveness is observed to depend on the radiation quality (e.g., the LET), dose rate, and dose fractionation, as well as the type and magnitude of the biological endpoint measured. RBE values vary markedly, depending upon these conditions.

The dependence of relative biological effectiveness on radiation quality is often discussed in terms of the LET of the radiation, or the LET of the secondary charged particles produced in the case of photons and neutrons. As a general rule, RBE increases with increasing LET, as illustrated in Fig. 13.15, up to a point. Figure 13.16 represents schematically the RBE for cell killing as a function of the LET of charged particles. Starting at low LET, the efficiency of killing increases with LET, evidently because of the increasing density of ionizations, excitations, and radicals produced in critical targets of the cell along the particle tracks. As the LET is increased further, an optimum range around 100 to 130 keV μm^{-1} is reached for the most efficient pattern of energy deposition by a particle for killing a cell. A still further increase in LET results in the deposition of more energy than needed for killing, and the RBE decreases. Energy is wasted in this regime of overkill at very high LET.

The most relevant values of RBE for purposes of radiation protection are those for low doses and low dose rates. For most endpoints, the RBE increases with decreasing dose, as seen in Fig. 13.15, and dose rate. In the context of the linear-quadratic dose–response model illustrated in Fig. 13.12, this increase in the RBE ratio as defined by Eq. (13.19) is associated almost entirely with the decrease in the slope of the curve for the low-LET reference radiation. The maximum values of the RBE determined in this region are denoted by RBE_M.[9)] For a given radiation and endpoint, RBE_M is thus equal to the ratio of the slope of the dose–response curve H in Fig. 13.12 for the radiation and the slope of L_2 from the linear portion of the low-LET reference radiation (e.g., X rays). We shall return to the subject of RBE_M in the next chapter on exposure limits. Table 13.8 summarizes estimates of RBE_M for fission neutrons relative to X rays.

7 NCRP Report No. 104, p. 27 (see references, Sect. 13.15).

8 C. J. Shellabarger, D. Chmelevsky, and A. M. Kellerer, "Induction of Mammary Neoplasms in the Sprague-Dawley Rat by 430 keV Neutrons and X Rays," *J. Nat. Cancer Inst.* **64**, 821 (1980).

9 For stochastic effects. For deterministic effects, the maximum is denoted by RBE_m. See ICRP Publication 58, *RBE for Deterministic Effects*, Pergamon Press, Elmsford, N.Y. (1990).

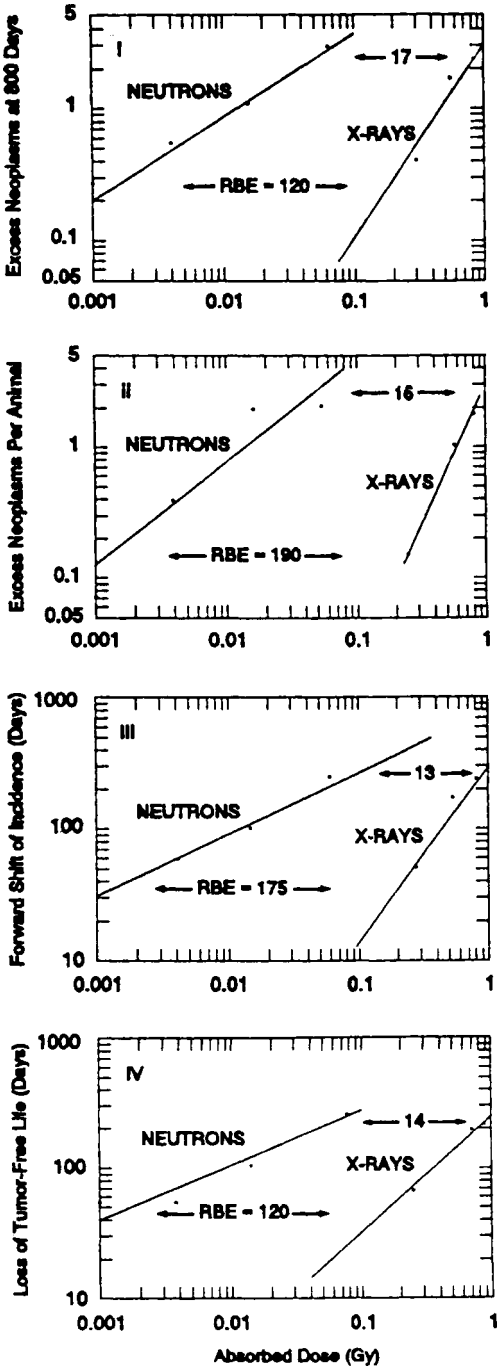

Fig. 13.15 Examples of dose–response curves for irradiation of Sprague-Dawley rats by X rays and 430-keV neutrons (see text).

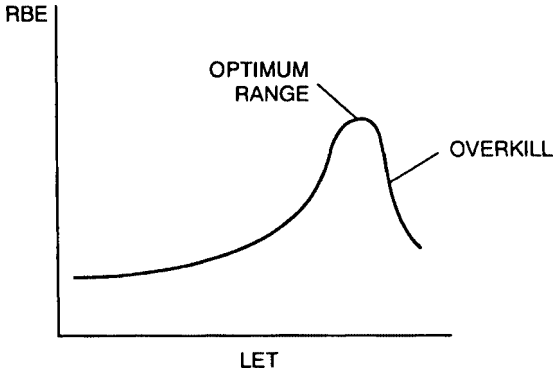

Fig. 13.16 Schematic representation of RBE for cell killing by charged particles as a function of their LET.

Table 13.8 Estimated RBE_M Values for Fission Neutrons and X Rays

Endpoint	Range
Cytogenic studies, human lymphocytes in culture	34–53
Transformation	3–80
Genetic endpoints in mammalian systems	5–70
Genetic endpoints in plant systems	2–100
Life shortening, mouse	10–46
Tumor induction	16–59

Source: From NCRP Report No. 104 (see references, Section 13.15).

Dose Rate

The dependence of dose–response relationships on dose rate has been demonstrated for a large number of biological effects. In Section 13.11 we mentioned the role of repair mechanisms in reducing the mutation frequency per Gy in mice when the dose rate is lowered. Another example of dose-rate dependence is shown in Fig. 13.17. Mice were irradiated with ^{60}Co gamma rays at dose rates ranging up to several tens of Gy h^{-1} and the LD50 determined. It was found that LD50 = 8 Gy when the dose rate was several Gy h^{-1} or more. At lower dose rates the LD50 increased steadily, reaching approximately 16 Gy at a rate of 0.1 Gy h^{-1}. Evidently, animal cells and tissues can repair enough of the damage caused by radiation at low dose rates to survive what would be lethal doses if received in a shorter period of time.

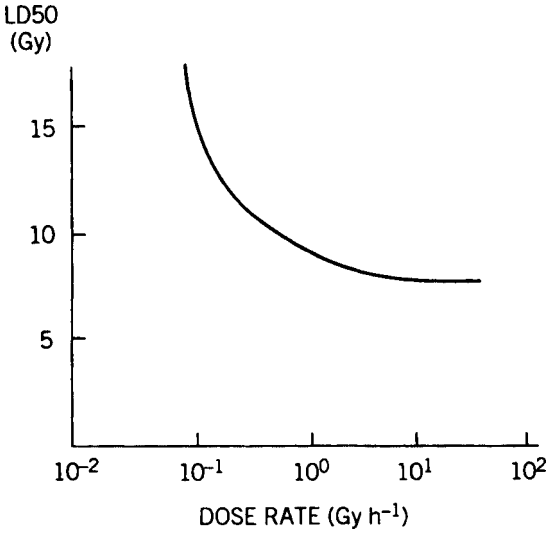

Fig. 13.17 Dependence of LD50 on dose rate for mice irradiated with ^{60}Co gamma rays. [Based on J. F. Thomson and W. W. Tourtellotte, *Am. J. Roentg. Rad. Ther. Nucl. Med.* **69**, 826 (1953).]

Oxygen Enhancement Ratio

Dissolved oxygen in tissue acts as a radio-sensitizing agent. This so-called oxygen effect, which is invariably observed in radiobiology, is illustrated in Fig. 13.18. The curves show the survival of cells irradiated under identical conditions, except that one culture contains dissolved O_2 (e.g., from the air) and the other is purged with N_2. The effect of oxygen can be expressed quantitatively by means of the oxygen enhancement ratio (OER), defined as the ratio of the dose required under conditions of hypoxia and that under conditions in air to produce the same level of effect. According to this definition, one would obtain the OER from Fig. 13.18 by taking the ratio of doses at a given survival level. OER values are typically 2–3 for X rays, gamma rays, and fast electrons; around 1.7 for fast neutrons; and close to unity for alpha particles.

The existence of the oxygen effect provides strong evidence of the importance of indirect action in producing biological lesions (Section 13.6). Dissolved oxygen is most effective with low- rather than high-LET radiation, because intratrack reactions compete to a lesser extent for the initial reaction product.

Chemical Modifiers

Chemicals which, like oxygen, have a strong affinity for electrons can make cells more sensitive to radiation. A number of radiosensitizing chemicals and drugs are known. Some sensitize hypoxic cells, but have little or no effect on normally aerated cells. Other agents act as radioprotectors, reducing biological effectiveness.

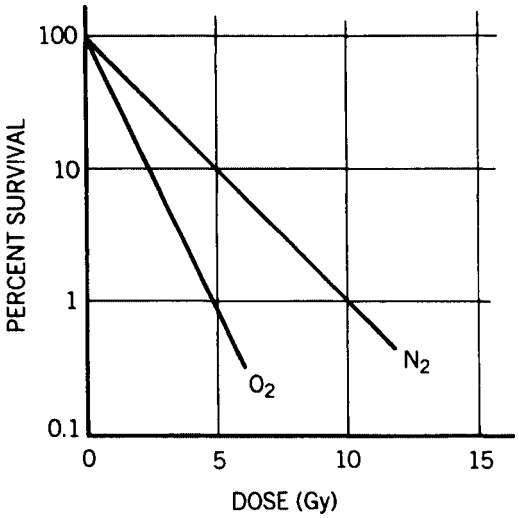

Fig. 13.18 Cell survival in the presence of dissolved oxygen (O_2) and after purging with nitrogen (N_2).

The most notable of these are sulfhydryl compounds (e.g., cysteine and cystamine), which scavenge free radicals. Still other chemical modifiers have little effect on cell killing, but substantially enhance some multistep processes, such as oncogenic cell transformation. For carcinogenesis or transformation, for example, such biological promoters can dwarf the effects of physical factors, such as LET and dose rate, on dose–response relationships.

Chemical radiosensitizers for use in radiation therapy are under investigation. Some have the potential to specifically affect resistant hypoxic cells, which are common in tumors. Chemical radioprotectors have been developed for potential military use in a nuclear war.

Dose Fractionation and Radiotherapy

The goal of treating a malignant tumor with radiation is to destroy it without damaging normal tissues to an intolerable degree. By and large, normal cells and tumor cells have comparable resistance to killing by radiation. Thus, other factors must come into play in radiotherapy. It is found empirically that the most advantageous results are obtained when the radiation is delivered to a patient in fractions, administered perhaps over a period of weeks, rather than all at once.

To understand how the fractionation of dose affects tumor cells more adversely than normal ones in a patient, there are basically four factors to consider at the cellular level: repair, repopulation, redistribution, and reoxygenation. Administering a dose in fractions with adequate time between applications allows the repair of sublethal damage and the repopulation of tissue cells. These processes generally occur on different time scales and to different degrees in the normal and tumor cells. The therapeutic protocol considers optimization of normal-tissue sparing to the detri-

ment of the tumor cells in prescribing the total dose, the number of fractions, the dose per fraction, and the total treatment time.

Because cells exhibit different degrees of radiosensitivity in different phases of the cell cycle, an asynchronous cell population will become partially synchronized by irradiation. The surviving cells will generally be those in the more resistant phases. As the population continues to grow following exposure, the partially synchronized surviving cells become redistributed over the complete cycle, including the more sensitive phases. This process of redistribution, combined with repeated irradiation at intervals, tends to result in increased cell killing relative to that achieved with a single dose.

The oxygen effect is extremely important in radiotherapy. Tumors often have poorly developed blood vessels, intermittent blood flow, and clonogenic cells with greatly reduced oxygen tension. They contain regions with viable cells, which are, however, hypoxic and therefore relatively resistant to radiation (cf., Fig. 13.18). Delivering radiation to a tumor in fractions allows reoxygenation of some hypoxic cells to occur between doses. As an added factor, sensitization increases rapidly with oxygen tension. The result is greater killing of tumor cells than with a comparable single dose. The response of the normal, oxygenated cells is unchanged by this procedure.

13.15 Suggested Reading

A vast amount of information is readily available on the World Wide Web, as well as complete copies (some searchable) of several of the works listed below.

1 Baverstock, K. F., and Stather, J. W., eds., *Low Dose Radiation, Biological Bases of Risk Assessment,* Taylor and Francis, London (1989). [This valuable book of 606 pages contains 54 contributions, covering all essential aspects of its subject. The articles are from scientists in a number of disciplines.]

2 BEIR V, *Health Effects of Exposure to Low Levels of Ionizing Radiation: BEIR V*, Committee on the Biological Effects of Ionizing Radiation, National Research Council, National Academy Press, Washington, DC (1990).

3 BEIR VI, *The Health Effects of Exposure to Indoor Radon: BEIR VI*, Committee on the Biological Effects of Ionizing Radiation, National Research Council, National Academy Press, Washington, DC (1999).

4 BEIR VII, *Health Risks from Exposure to Low Levels of Ionizing Radiation: BEIR VII–Phase 2*, Committee on the Biological Effects of Ionizing Radiation, National Research Council, National Academy Press, Washington, DC (2006). [Reviews health risks from exposure to low levels of low-LET ionizing radiation. Updates BEIR V. Detailed risk estimates for both cancer incidence and cancer mortality are given. Required reading.]

5 Glass, W. A., and Varma, M. N., eds., *Physical and Chemical Mechanisms in Molecular Radiation Biology*, Plenum Press, New York, NY (1991). [A collection of 18 papers at an invited workshop on the subject. Contributions are made from fields of radiological physics, radiation chemistry, and radiation-effects modeling.]

6 Gusev, Igor A., Guskova, Angelina, and Mettler, Fred A., eds., *Medical Management of Radiation Accidents,*

2nd Ed., CRC Press, Boca Raton, FL (2001).

7 Hall, Eric J., and Giaccia, Amato, J., *Radiobiology for the Radiologist*, 6th Ed., Lippincott Williams and Wilkins, Philadelphia, PA (2005).

8 Johns, H. E., and Cunningham, J. R., *The Physics of Radiology*, 4th Ed., Charles C. Thomas, Springfield, IL (1983). [Chapter 17, on radiobiology, is highly recommended.]

9 Mozumda, A., *Fundamentals of Radiation Chemistry*, Academic Press, San Diego, CA (1999).

10 NCRP Report No. 78, *Evaluation of Occupational and Environmental Exposures to Radon and Radon Daughters in the United States*, National Council on Radiation Protection and Measurements, Washington, DC (1984).

11 NCRP Report No. 103, *Control of Radon in Houses*, National Council on Radiation Protection and Measurements, Washington, DC (1989).

12 NCRP Report No. 104, *The Relative Biological Effectiveness of Radiations of Different Quality*, National Council on Radiation Protection and Measurements, Washington, DC (1990).

13 NCRP Proceedings 42nd Annual Meeting, April 3–4, 2006, *Chernobyl at Twenty, Health Phys.* in press.

14 Preston, R. Julian, "Radiation Biology: Concepts for Radiation Protection," *Health Phys.* 88, 545–556 (2005). [An important review article, one of the invited contributions in the volume commemorating the 50th anniversary of the Health Physics Society.]

15 *Radiation Research* **137** (Supplement), S1–S112 (1994). [A special issue devoted to cancer incidence in atomic-bomb survivors, Radiation Effects Research Foundation, Hiroshima, and Nagasaki, Japan.]

16 *Radiation Research* **161**, No. 4, April 2004, "A Cohort Study of Thyroid Cancer and Other Thyroid Diseases after the Chornobyl Accident: Objectives, Design and Methods."

17 Ricks, R. C., Berger, Mary Ellen, and O'Hara, Frederick M., Jr., Eds., *Proceedings of the Fourth International REAC/TS Conference on the Basis for Radiation Accident Preparedness*, CRC Press, Boca Raton, FL (2001).

18 Sagan, L. A., Guest Editor, *Health Phys.* **52**, 250-680 (1987). [Special issue on radiation hormesis.]

19 Smith, Jim T., and Beresford, Nicholas A., *Chernobyl—Catastrophe and Consequences*, Springer, Secaucas, NJ (2005).

20 Sugahara, T., Sagan, L. A., and Aoyama, T., eds., *Low Dose Irradiation and Biological Defense Mechanisms*, Excerpta Medica International Congress Series 1013, 526 pp., Pergamon Press, Elmsford, NY (1992). [Proceedings of the subject conference, held in Kyoto, Japan in July, 1992. The presentations furnish an overview of the state of knowledge regarding effects of low levels of radiation and radiation hormesis.]

21 United Nations Scientific Committee on the Effects of Atomic Radiation (UNSCEAR), *Sources and Effects of Ionizing Radiation*, UNSCEAR 2000 Report to the General Assembly, United Nations Publications, New York (2000). [In two volumes, 1,300 pp.: Vol. 1, Sources; Vol. 2, Effects.]

13.16 Problems

1. What initial changes are produced directly by ionizing radiation in water (at $\sim 10^{-15}$ s)?

2. What reactive species exist in pure water at times $>10^{-12}$ s after irradiation?
3. Do all of the reactive species (Problem 2) interact with one another?
4. Estimate how far an H_3O^+ ion will diffuse, on the average, in water in 5×10^{-12} s.
5. Estimate the average time it takes for an OH radical to diffuse 400 Å in water.
6. If an OH radical in water diffuses an average distance of 3.5 Å in 10^{-11} s, what is its diffusion constant?
7. Estimate how close an H_3O^+ ion and a hydrated electron must be to interact.
8. How far would a water molecule with thermal energy (0.025 eV) travel in 10^{-12} s in a vacuum?
9. If a 20-keV electron stops in water and an average of 352 molecules of H_2O_2 are produced, what is the G value for H_2O_2 for electrons of this energy?
10. If the G value for hydrated electrons produced by 20-keV electrons is 1.13, how many of them are produced, on the average, when a 20-keV electron stops in water?
11. What is the G value for ionization in a gas if $W = 30$ eV ip^{-1} (Section 10.1)?
12. Use Table 13.3 to find the average number of OH radicals produced by a 500-eV electron in water.
13. For what physical reason is the G value for H_2 in Table 13.3 smaller for 20-keV electrons than for 1-keV electrons?
14. Why do the G values for the reactant species H_3O^+, OH, H, and e^-_{aq} decrease between 10^{-12} s and 10^{-6} s? Are they constant after 10^{-6} s? Explain.
15. For 5-keV electrons, the G value for hydrated electrons is 8.4 at 10^{-12} s and 0.89 at 2.8×10^{-7} s. What fraction of the hydrated electrons react during this period of time?
16. **(a)** Why are the yields for the reactive species in Table 13.4 for protons greater than those for alpha particles of the same speed?
    (b) Why are the relative yields of H_2 and H_2O_2 smaller?
17. A 50-cm^3 sample of water is given a dose of 50 mGy from 10-keV electrons. If the yield of H_2O_2 is $G = 1.81$ per 100 eV, how many molecules of H_2O_2 are produced in the sample?
18. Assume that the annual exposure of a person in the United States to radon daughters is 0.2 WLM. Use the BEIR-IV estimated lifetime risk of 350 excess cancer deaths per 10^6 person WLM to predict the annual number of such deaths in a population of 250 million people.

19. Distinguish between the "direct" and "indirect" effects of radiation. Give a physical example of each.

20. Give examples of two stochastic and two deterministic biological effects of radiation.

21. What are the major symptoms of the acute radiation syndrome?

22. Given the tenet that the most rapidly dividing cells of the body are the most radiosensitive, show how it is reflected in the information given in Table 13.6 for the acute radiation syndrome.

23. What are the principal late somatic effects of radiation? Are they stochastic or deterministic?

24. According to the BEIR V Report, an acute, whole-body, gamma-ray dose of 0.1 Gy to 100,000 persons would be expected to cause about 800 extra cancer deaths in addition to the 20,000 expected naturally.

(a) If an "experiment" could be carried out to test this risk estimate for a dose of 0.1 Gy, would a population of 10,000 individuals be sufficiently large to obtain statistically significant results?

(b) A population of 100,000?

(c) What kind of statistical distribution describes this problem?

25. Show that D_0 in Eq. (13.16) is the mean lethal dose.

26. Survival of a certain cell line exposed to a beam of helium ions is described by the single-target, single-hit model and Eq. (13.16). If 25% of the cells survive a fluence of 4.2×10^7 cm^{-2}, what is the single-target area?

27. Justify the use of Poisson statistics in arriving at Eqs. (13.16) and (13.17).

28. Why do experiments that seek to quantify dose–effect relationships at low doses require large exposed and control populations?

29. Cell survival in a certain set of experiments is described by the function $S/S_0 = e^{-3.1D}$, where D is the dose in Gy.

(a) What is the mean lethal dose?

(b) What is the LD50?

(c) What is the difference between LD50 and mean lethal dose?

30. If 41 Gy reduces the exponential survival of cells to a level of 1%, what is the mean lethal dose?

31. For multitarget, single-hit survival with $D_0 = 7.5$ Gy and an extrapolation number $n = 4$, what fraction of cells survive a dose of 10 Gy?

32. Repeat Problem 31 for $D_0 = 7.5$ Gy and $n = 3$.

33. Repeat Problem 31 for $D_0 = 5.0$ Gy and $n = 4$.

34. What interrelationships do the extrapolation number, the magnitude of D_0, and the size of the shoulder have in a multitarget, single-hit cell-survival model?

35. Why does survival in a multitarget, single-hit model become exponential at high doses?

36. **(a)** Sketch a linear plot of the exponential survival curve from Fig. 13.13.
(b) Sketch a linear plot for the multitarget, single-hit curve from Fig. 13.14. What form of curve is it?

37. A multitarget, single-hit survival model requires hitting n targets in a cell at least once each to cause inactivation. A single-target, multihit model requires hitting a single target in a cell n times to produce inactivation. Show that these two models are inherently different in their response. (For example, at high dose consider the probability that hitting a target will contribute to the endpoint.)

38. One can describe the exponential survival fraction, S/S_0, by writing $S/S_0 = e^{-pD}$, where D is the number of "hits" per unit volume (proportional to dose) and p is a constant, having the dimensions of volume. Show how p can be interpreted as the target size (or, more rigorously, as an upper limit to the target size in a single-hit model).

39. The cell-survival data in Table 13.9 fit a multitarget, single-hit survival curve. Find the slope at high doses and the extrapolation number. Write the equation that describes the data.

40. Cell survival is described in a certain experiment by the single-target, single-hit response function, $S/S_0 = e^{-1.6D}$, where D is in Gy. At a dose of 1 Gy, what is the probability of there being
(a) no hits
(b) exactly two hits in a given target?

Table 13.9 Data for Problem 39

Dose (Gy)	Surviving Fraction
0.10	0.993
0.25	0.933
0.50	0.729
1.00	0.329
2.00	0.0458
3.00	0.00578
4.00	0.00072

41. A colony of identical cells (unit density) is irradiated with neutrons, which deposit an average of 125 keV of energy in a collision. A single neutron collision in a sensitive volume of a cell inactivates the cell.

(a) If a dose of 0.50 Gy inactivates 11 % of the cells, what is the average number of neutron collisions in the sensitive volume of a cell in the colony?

(b) What is the size of the sensitive volume of a cell in μm^3?

(c) What fraction of the cells are expected to be inactivated by a dose of 2.0 Gy?

42. The survival of a certain cell line when exposed to X rays is found experimentally to be described by the equation

$$\frac{S}{S_0} = 1 - (1 - e^{-0.92D})^2,$$

where D is in Gy. Survival of the same cell line exposed to neutrons is described by

$$\frac{S}{S_0} = e^{-0.92D},$$

with D in Gy.

(a) What is the RBE for the neutrons (relative to the X rays) for 10% survival of the cells?

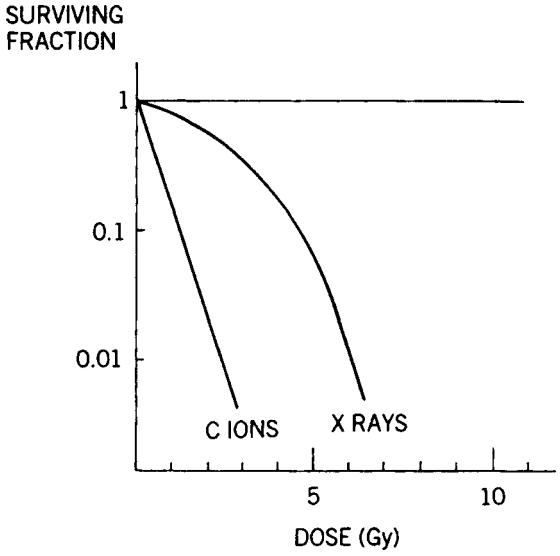

Fig. 13.19 Surviving fraction of cells as a function of dose (Problem 44).

(b) At a higher level of survival (lower dose), is the RBE larger or smaller?

(c) Give a reason to explain your answer to (b).

43. What factors can modify dose–effect relationships?

44. Figure 13.19 shows the surviving fraction of cells as a function of dose when exposed to either X rays or carbon ions in an experiment. From the curves, estimate the RBE of the carbon ions for 1% survival and for 50% survival. What appears to happen to the RBE as one goes to lower and lower doses?

45. Explain why radiation is used in cancer therapy, even though it kills normal cells.

46. Estimate the oxygen enhancement ratio from the cell-survival curves in Fig. 13.18.

47. Are the curves in Fig. 13.18 more typical of results expected with high-LET or low-LET radiation? Why?

13.17 Answers

4. 4.9 Å

5. 1.3×1^{-7} s

7. 2.4 Å

8. 5.2 Å

11. 3.3

12. 2.3

15. 0.89

17. 2.83×10^{14}

18. 17,500

26. 3.3 μm^2

31. 0.706

41. **(a)** 0.117

(b) 4.68 μm^3

(c) 0.373

42. **(a)** 1.3

(b) Larger

44. 2.7, 5.3

46. 2.0